4. METEOROLOGICAL MODELING

The project team employed the Regional Atmospheric Modeling System (RAMS) and the PSU/NCAR Mesoscale Model version 5 (MM5) to develop the meteorology for the SFBA ozone episodes (plus initialization days). As the primary model of choice at the start of this project, RAMS was the first of these models to be applied in numerous simulations of all three episodes based on the CCOS grid structure defined by the CARB. Near the midpoint of the project, the BAAQMD acquired additional staff with experience in running MM5; given the promising photochemical modeling results achieved by CARB using MM5 meteorology at the time, the BAAQMD began their own intensive MM5 modeling campaign in parallel with the ATMET RAMS applications.

This section briefly describes both models, and summarizes their application and performance against observed conditions. Further details on the RAMS modeling configuration, simulations, and performance results are fully described in the RAMS meteorological modeling final report for this project (ATMET, 2004). The ATMET report also provides a general discussion on the observed synoptic and local meteorological patterns that set up during both the July/August 2000 and July 1999 episodes.

RAMS APPLICATIONS

ATMET used RAMS to simulate the meteorology for the three ozone episodes described in Section 2: July/August 2000, June 2000, and July 1999. Only the first and third episodes will be addressed here. The meteorological situation that occurred during the June 2000 episode proved difficult to simulate with RAMS. Ultimately, the June 2000 episode was dropped from further consideration in this project for several reasons: (1) we felt that the performance of the RAMS simulations did not meet our normal standards (MM5 was never applied to this episode); (2) as one of two "Type 2" episodes (see Section 2) it effectively duplicated the ozone conditions observed in the more intensively monitored July/August 2000 CCOS episode; and (3) this episode has not been a priority for CARB in any CCOS modeling performed for other areas in California. The June 2000 episode will not be discussed further in this report.

Description of RAMS

RAMS has been developed by a number of groups since its inception, including Colorado State University (CSU) and Mission Research Corporation (MRC). With the changes over the past two years, the primary focus of development has been at ATMET and Duke University, although CSU and MRC are still involved. RAMS is a multipurpose, numerical prediction model that simulates atmospheric circulations ranging in scale from an entire hemisphere down to large eddy simulations (LES) of the planetary boundary layer. It is most frequently used to simulate atmospheric phenomena on the mesoscale (horizontal scales from 2 km to 2000 km) for applications ranging from operational weather forecasting to air quality applications to support of basic research. RAMS has often been successfully used with much higher resolutions to simulate boundary layer eddies (10-100 m grid spacing), individual building simulation (1 m grid spacing), and direct wind tunnel simulation (1 cm grid spacing). RAMS predecessor codes were developed to perform research in modeling physiographically-driven weather systems and

simulating convective clouds, mesoscale convective systems, cirrus clouds, and precipitating weather systems in general. RAMS use has continued to increase to more than 200 current RAMS installations in more than 40 different countries. Although RAMS is supported on all UNIX, Linux, and Windows platforms, because of the exceptional price/performance ratios, we are recently focusing on Linux PCs and PC clusters as our primary computational platform.

The current version of RAMS that is released to the general RAMS user community is version 4.4. We anticipate that version 5.0 will be released in late 2004. Along with an upgrade of the RAMS code structure to more modern and safer FORTRAN 90 constructs, during the time frame of this project, the following features were added to the v5.0 RAMS code:

- Generalized observational-nudging 4DDA scheme
- Urban canopy parameterization
- Antecedent precipitation index scheme for soil moisture initialization
- Several diabatic initialization options
- Use of NDVI datasets to define vegetation characteristics

Additional information about the model's capabilities is provided in ATMET (2004).

RAMS Configuration

ATMET used the latest versions of RAMS (v5.0) for the simulations. Comparisons performed with the officially-released version (v4.4) on this and other projects showed that the two versions compared well when configured in the same manner. By moving to v5.0, we had access to the numerous new features and improvements that have been implemented.

The RAMS horizontal grid structure was configured as similarly as possible to the emissions, MM5, and CAMx modeling domain specified by CARB for CCOS modeling (Figure 4-1). Note that RAMS does not operate on the Lambert conic conformal projection employed by CCOS. However, care was taken to closely coordinate the RAMS and MM5/CAMx grid resolution and domain coverage to minimize the impact of interpolation errors, and to better ensure mass consistency, in the transfer of the meteorological fields from RAMS to CAMx. Specifically, the rotated polar stereographic projection in RAMS was centered at the same geodetic coordinates as the central coordinates of the CARB's MM5 Lambert projection. This minimizes projection differences to within tolerable error out to the edges of the grid. We used both a 3-grid (finest grid with 4-km spacing) and a 4-grid (finest grid with 1-km spacing) configuration for the episodes. Surrounding the finer grids was a 12-km nest, which in turn was nested within a 48-km grid to resolve the large scale forcing (Figure 4-2 and Table 4-1). All grids are run in RAMS in 2-way nesting mode, meaning information propagates up- and down-scale among all grids simultaneously during a simulation.

For the vertical structure, RAMS was configured to run all grids with 41 coordinate levels, with the lowest wind and temperature level at about 15 m AGL, then smoothly stretching to a maximum of about 1000 m grid spacing (Figure 4-3). The top of the model was placed at about 20 km MSL to ensure that the various synoptic scale features such as the sub-tropical jet stream (which is located about tropopause level) were adequately resolved in the simulation domain. Although the upper level jets are not directly important in the low-level transport of ozone and its

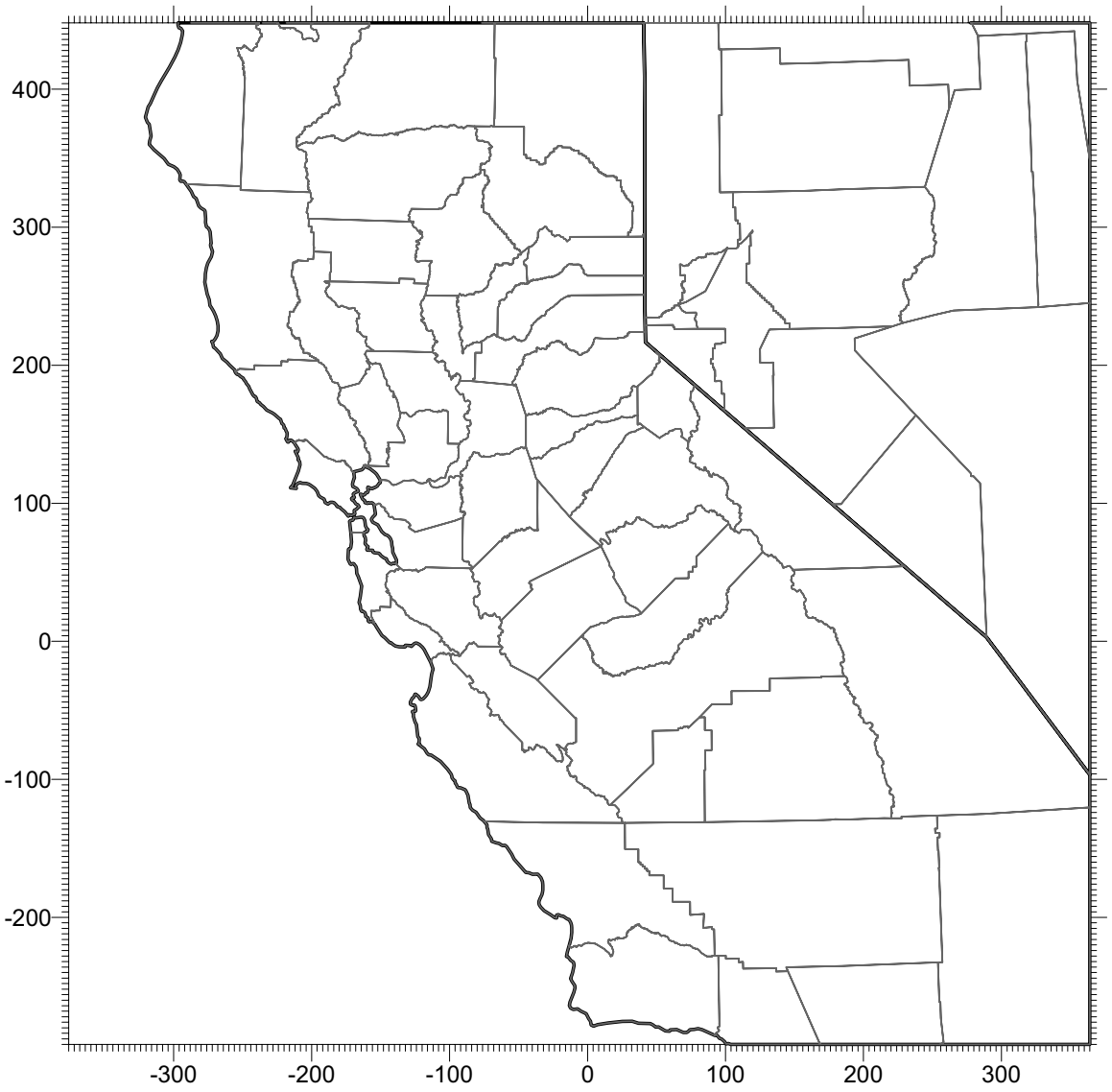

Figure 4-1. The coverage of the CARB/CCOS air quality modeling domain. Grid spacing over the entire region is 4 km. Map projection is Lambert Conformal.

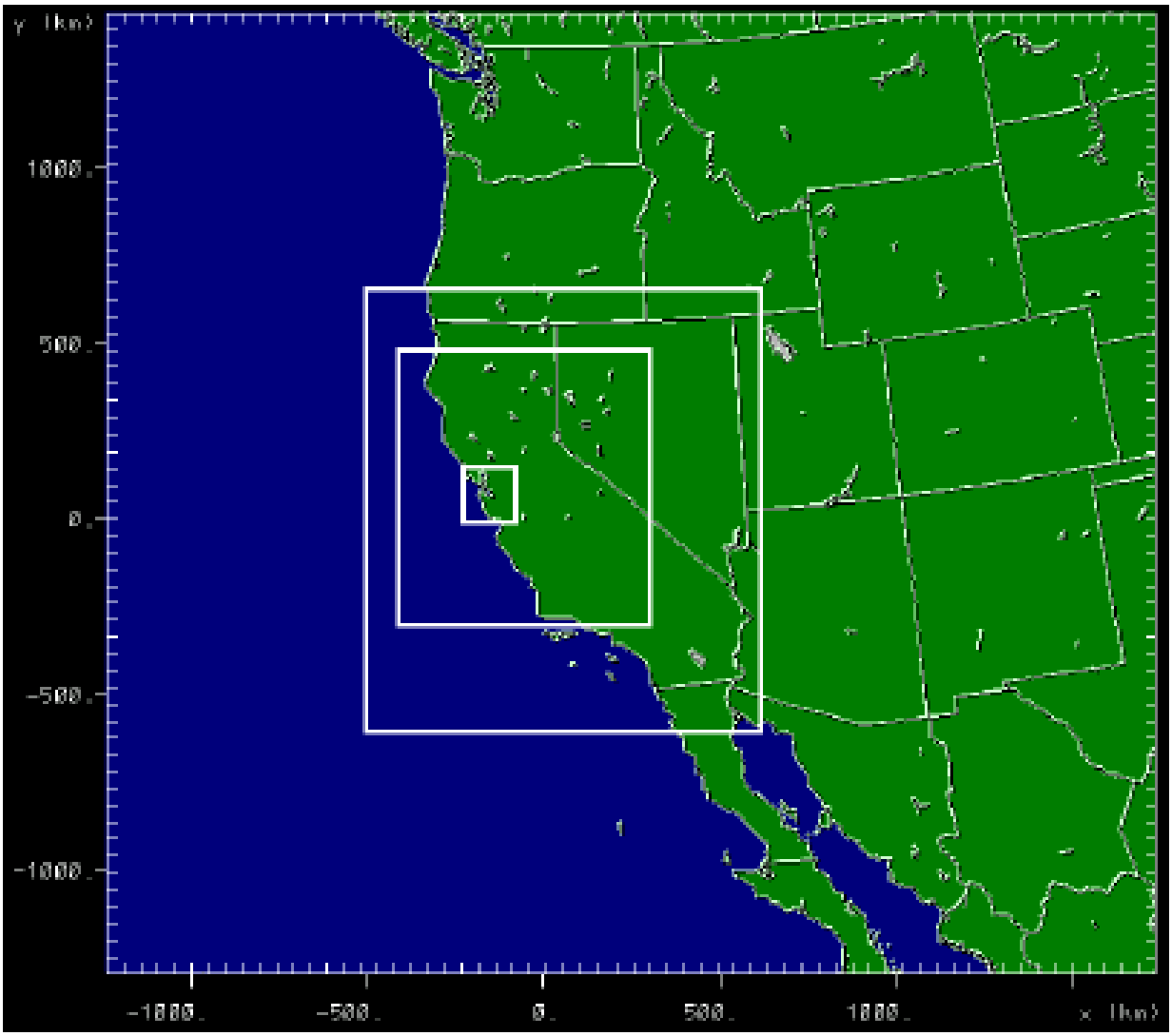

Figure 4-2. Depiction of the RAMS rotated polar stereographic modeling grid configuration, which employed a system of up to four nested grids with successively finer resolution.

Table 4-1. Grid parameters for each of the nested domains shown in Figure 4-2.

Grid	# of X points	# of Y Points	Vertical Levels	Δx (km)	Δy (km)	Δz (m) (Lowest)	Δt (s)
1	63	58	41	48	48	15	60
2	94	106	41	12	12	15	30
3	179	197	41	4	4	15	15
4	150	158	41	1	1	15	7.5

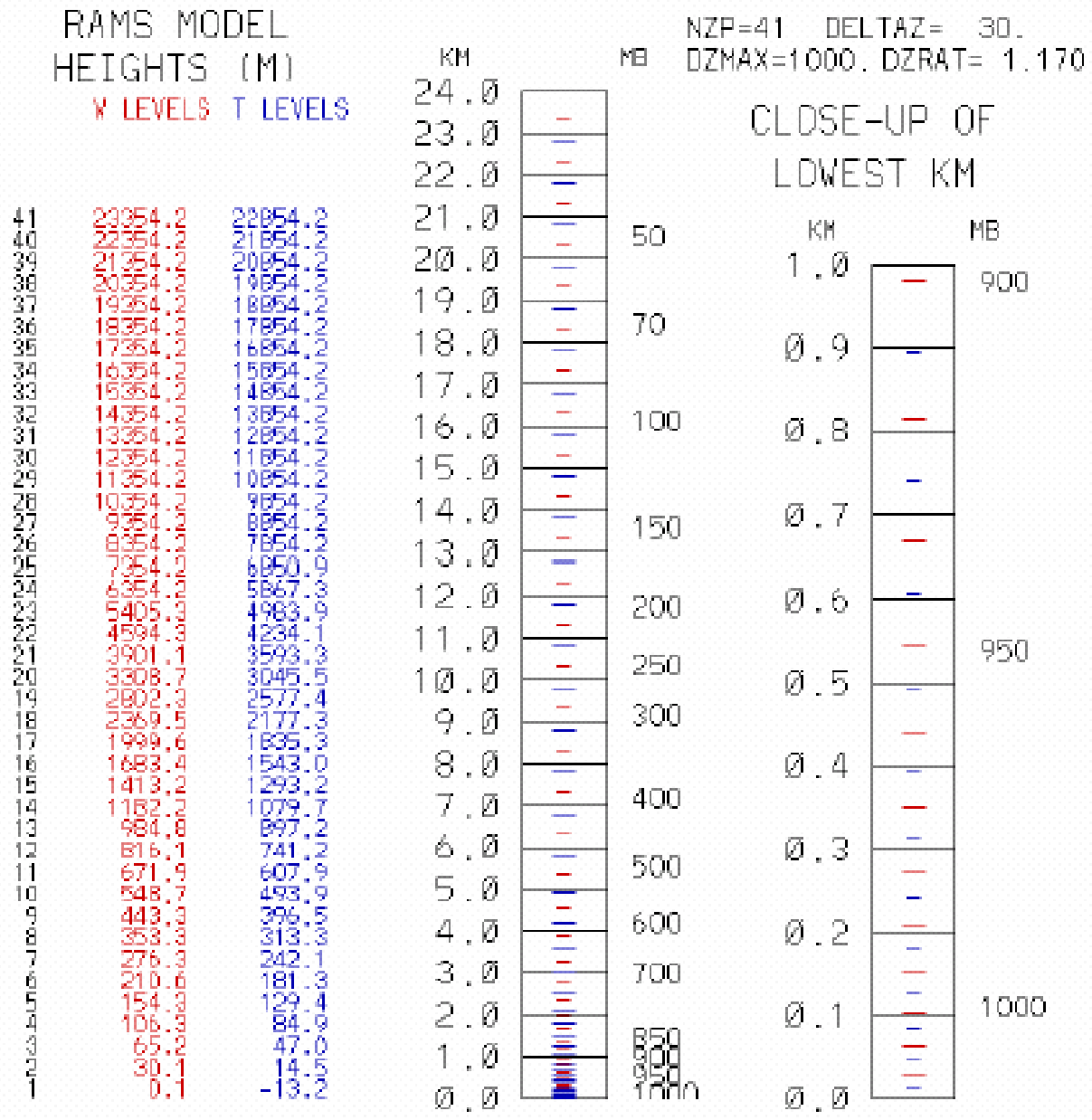

Figure 4-3. Vertical grid structure used for RAMS.

precursors, the jets do affect tropospheric dynamics and low-level pressure patterns, which control the low-level winds.

RAMS was configured with the following physical and numerical options for these simulations:

- Mellor-Yamada type subgrid diffusion based on a prognostic turbulent kinetic energy;
- Long and short wave radiative parameterizations (sensitivity runs performed with different schemes);

- Land surface model: prognostic soil temperature/moisture and vegetation parameterization (LEAF3);

- Full microphysics parameterization (5 ice and 2 liquid species, prognostic ice nuclei concentration);

- Convective parameterization (Kuo-type);

- Four-dimensional data assimilation (analysis and observational nudging).

The four-dimensional data assimilation (FDDA) scheme, which has been used in the past by RAMS for these types of simulations, has been termed in the meteorological literature as "analysis nudging". However, in certain circumstances, "observational nudging" has some advantages. With the new observational nudging scheme that has been implemented in RAMS v5.0, we had the ability to exercise and test the sensitivity to both types of FDDA schemes.

Input Data

Meteorological Data

The input meteorological data for the simulated episodes were derived from standard NWS observation datasets along with the available the available mesonet/CCOS observations. The meteorological input data to the meteorological models can be grouped into three categories:

1) Large scale gridded analyses: Various datasets are available from the National Centers for Environmental Prediction (NCEP) and NCAR. For the July/August 2000 episode, we used the NCEP/NCAR Reanalysis data. In this dataset, the parameters of wind, temperature, and humidity are analyzed on pressure levels (20 levels extending from 1000 mb up to 10 mb) on a 2.5 degree latitude-longitude grid. These data are archived every 6 hours and serve as a first guess field for the data analysis. We accessed this data from the National Center for Atmospheric Research (NCAR). For the July 1999 episode, we used the EDAS (ETA Data Assimilation System) data, which is the data analysis produced as the initial conditions for the ETA forecasts at NCEP.

2) Standard NWS observations: The rawinsondes and surface observations reported by the NWS and other national meteorological centers are also archived at NCAR. The rawinsondes are reported every 6 hours and the surface observations are archived every hour. These data were accessed for all simulated days.

3) Special observations: Special observations taken during the summer of 2000 from the CCOS monitoring sites were included in the data analyses and FDDA for the July/August 2000 episode. These observations included surface observations, wind profilers, rawinsondes, etc. For the July 1999 episode, data from several of the same mesonets included in CCOS were acquired.

Topographic Data

Topography was defined from the RAMS standard input dataset, the USGS global 30 sec resolution (about 1 km) topographic dataset. A " normal" amount of smoothing was applied to each of the four grids. In RAMS, the smoothing is wavelength-specific and was defined to remove all wavelengths less than $4\Delta x$.

However, with this level of smoothing, the steepness of topography in the southeast quadrant of grid 3 (the extreme southeast Sierras) was exceeding the allowable changes in one grid space. All terrain-following coordinate models have limitations in this regard. Therefore, we implemented a regional smoother to smooth the topography only in this are. Since this region was adequately far from the Bay Area, this topographic smoothing did not affect the local Bay circulations.

Landuse/Landcover Data

The land use classifications for all grids were derived from a USGS 30 second global dataset. The original dataset has 93 categories. These were translated to the RAMS/LEAF 21 categories. Each RAMS grid cell used 3 different land use types, or patches. The first patch contains any water area, the second and third contain the first two most prevalent land use types as derived from the USGS data.

Along with the land use type itself, RAMS uses numerous other characteristics of the vegetation, including fractional coverage, albedo, and roughness length. The new RAMS v5.0 contains parameterizations to derive these quantities based on the land use type and NDVI (Normalized Difference Vegetation Index), which is available at the same resolution (different projections) as the global land use dataset.

Initial processing of the land use dataset showed that there was a significant coverage of irrigated cropland designation for the central valley. By default in RAMS, this designation is initialized to a very moist soil moisture content. In the real world, the state of the soil moisture is obviously highly dependent on the specific time of the year and if the irrigation is occurring at any given time on any given property. Unfortunately, no records are kept of the irrigation history of past time periods, so there is no way of knowing if, or what areas, may have been actively irrigating during these specific weeks in 1999-2000. However, several initial sensitivity experiments were run using the default initialization and showed too moist and too cool verifications for most of the central valley stations. This is a good indication that the soil was too moist. Therefore, we changed the landuse categorization from irrigated to non-irrigated crop for all locations and initialized the soil moisture according to the input parameters as described in the RAMS report (ATMET, 2004).

Water Surface Temperature

A typical first guess at initializing the ocean/bay/lake temperatures for a simulation is to use a 1º resolution, global climatological dataset. This dataset was originally produced by the Navy and encompasses a 30-year average from 1955-1985. An additional dataset was accessed from NCAR, a weekly OI global SST analysis (dataset ds277.0). The optimum interpolation (OI) sea

surface temperature (SST) analysis is produced on a 1º grid. The analysis uses in-situ and satellite SST's plus SST's simulated by sea-ice cover. The temperatures from the weekly SST analysis were within 1°C of the RAMS climatological SST.

Neither of these datasets have the resolution to accurately depict the water temperatures of San Francisco Bay. SFBA water temperature data are available from the USGS via the Water Quality of San Francisco Bay Website (http://sfbay.wr.usgs.gov/access/wqdata), and water temperature data were collected during two cruises in July and August 2000. Tabular data are also available from the website for more exact values. The water temperatures within the Bay varied from almost 22°C at the far south end of the Bay to about 16.5°C near the Bay entrance to about 19.5°C at the north end of the bay and then close to 22°C in the smaller bays upstream.

Sensitivity experiments (as described by ATMET [2004]) showed very little sensitivity of the surface fields on the actual bay water temperature. Additionally, Bay temperature measurements from June 2000 and July 1999 had very similar temperatures and patterns to those in July/August 2000. Therefore, for simplicity, we selected an average temperature of 19ºC for the bay and used this value for all three episodes.

Simulations of July/August 2000

This episode was the first simulated with RAMS. As such, various decisions concerning model configuration were needed to properly replicate the unique conditions within the CCOS region. Nearly twenty simulations were made to adjust various aspects of the configuration and to identify the overall best performing set up. Many of these were shorter simulations to test the sensitivities to various inputs and assumptions, mainly in regards to surface characteristics (soil moisture, landuse, water surface temperature, etc.). When performing the sensitivity studies, we usually perform the simulations in an incremental approach, in an attempt to understand the underlying causes for any differences in the results. The short term tests were run to get a good idea of the appropriate surface characteristics and then expanded into longer term simulations of the entire episode.

Selection of the Best Configuration

ATMET computed standard statistical performance measures over different portions of the domain, each area identified by CARB for its unique location and micro-climate (Figure 4-4). For the consideration of the " best" runs for this episode, we focused on statistics comparing modeled scalar and vector wind speed, temperature and dewpoint against standard hourly NWS surface station data located in central California (centered on the Bay Area). ATMET received the quality-assured special CCOS observation dataset very late in the project. The CCOS surface observation dataset was archived and produced by CARB and quality-assured by both BAAQMD and CARB. All of the RAMS runs were made using only the NWS data in the analyses for initial/boundary conditions and analysis nudging, while some of the later runs used the CCOS datasets in the observational nudging procedures and for some statistical evaluations. For all statistical performance evaluations, ATMET did not attempt any vertical reduction scheme to extrapolate RAMS-predicted values to station observation height, but simply compared the lowest layer simulated values (representative of 30 m deep layer average) directly to the observational data.

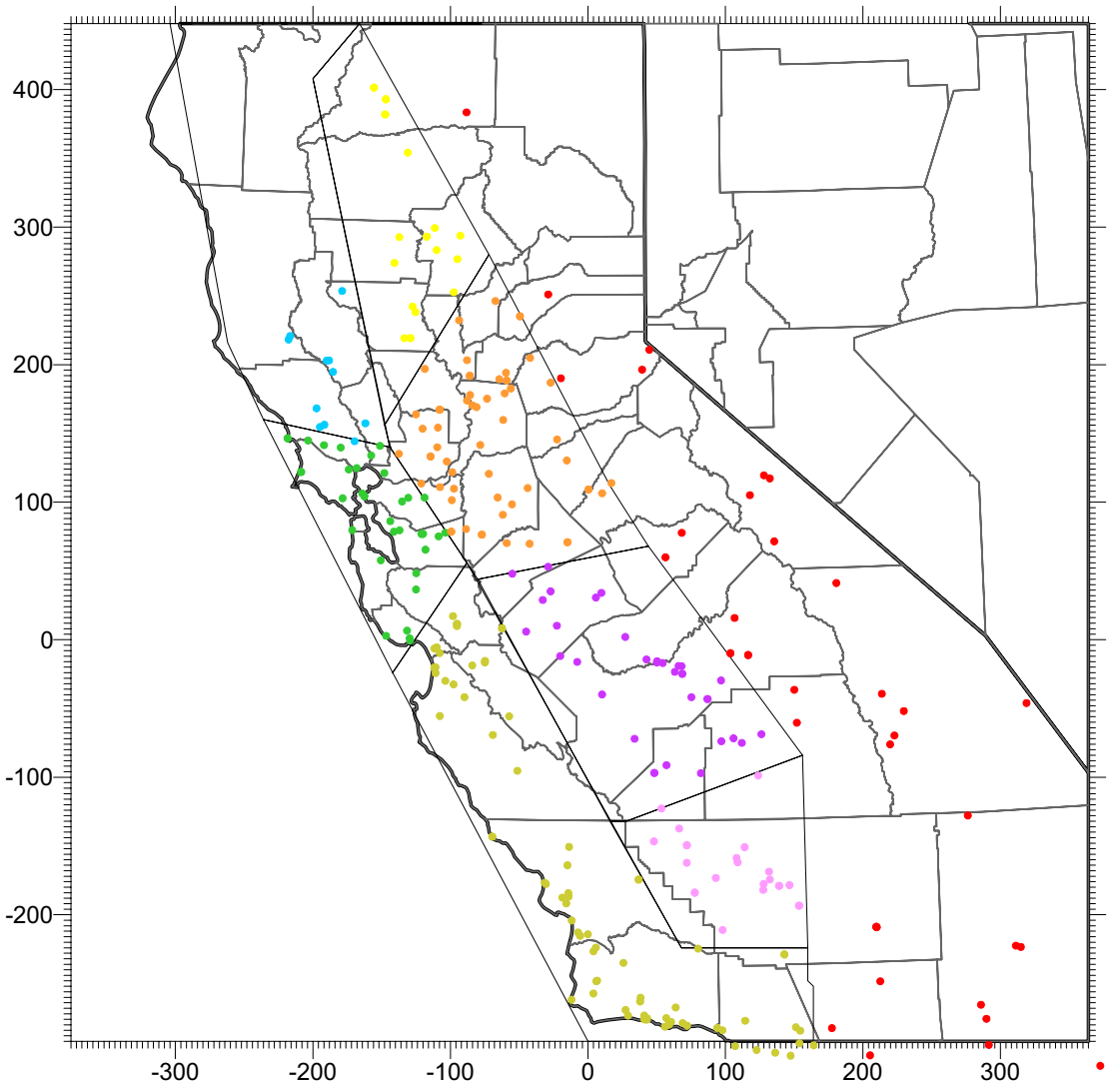

Figure 4-4. Locations of meteorological observation sites within the CCOS database. Site colors show the break out of these sites within each sub-regional analysis zone. These sites include NWS, AIRS, CIMIS, RAWS, certain private networks, and special CCOS intensive operating sites.

Because of our incremental testing approach, the later RAMS runs did have better performance than the early runs. Therefore, for sake of brevity, we will not discuss the statistics of the early simulations here. The best performing 3-grid runs (48/12/4-km nested grids) included those labeled as follows:

- W3: "medium" initial soil moisture content, relatively weak 3-D analysis nudging, 19°C bay surface temperature;
- O3: as in W3, but with surface observation nudging to NWS wind observations;
- W3O: as in O3, but with surface observation nudging to all CCOS wind observations.

In all three runs, there was a small warm, dry bias in the late afternoon hours with a mean relative error of about +1°C temperature and about -2°C dewpoint. The minimum temperatures at sunrise showed very little bias with a mean absolute error of 1-1.5°C or less. Wind

performance was quite good, matching the mean diurnal profiles quite well overall. Note, however, that run W3O used the CCOS datasets for the observational nudging and that this led to a low speed bias in the afternoon hours relative to NWS observations. We will explore the reasons for this in more detail when we discuss the 4-grid runs below.

The two best runs statistically for the 4-grid configuration were:

- W4: as in W3, but adding the high-resolution 1-km grid over the Bay Area (used Chen longwave radiation scheme);
- W4O: as in W3O, but adding the high-resolution 1-km grid over the Bay Area (used Harrington longwave radiation scheme).

Similar patterns in the temperature and dewpoint statistics against NWS surface observations were apparent in the 4-grid runs as compared to the 3-grid runs, except there was cold bias at night in the W4O run. This was due to the use of the Harrington longwave radiation scheme in this run as opposed to the Chen longwave radiation in the W4 run. The wind speed behavior with the 4-grid runs showed that the mean speed was higher than the 3-grid runs. This was most likely due to the better resolution of the topographic features and enhanced channeling. In the 3-grid runs, W3 (no observation nudging) showed close agreement with the NWS observed speeds in the afternoon hours, while W3O (observation nudging to CCOS data) showed an under prediction. In the 4-grid runs, W4 (no observation nudging) showed an over prediction while W4O agreed very well with the mean NWS values.

ATMET (2004) further examined the difference between runs without observational nudging and those with observational nudging separately to the NWS and CCOS data. Runs with observational nudging to the CCOS dataset consistently led to lower wind speeds. The wind speed statistics were repeated for W4O, but instead of verifying against the NWS surface observations, certain CCOS observations were used. The RAMS statistics were re-computed by excluding all stations identified as possessing 2 meter probe heights, since the RAMS' winds used in this comparison were representative of a layer mean height of about 15 meters. There were approximately 300 total stations in the complete CCOS dataset; about 105 stations were explicitly identified as "2 meter" sites.

ATMET found that the afternoon mean observed winds in the Bay Area computed from the reduced CCOS dataset were consistently lower than the mean observed wind speed computed from the NWS stations. While the RAMS W4O simulation, which did use all CCOS station data (with no regard to probe height), verified quite well against the NWS stations, there was a small over prediction of wind speed as compared to the CCOS stations. If in fact the heights of the observations were correctly described, we have no explanation for why there was such a discrepancy between the CCOS and NWS mean wind speeds. However, we do know that there were some significant differences in the station sitings; NWS sites are primarily at airports, while the AIRS sites are primarily grouped in urban areas and some are even located on top of buildings (leading to the potential for lower wind speeds). Also, other mesonets compiled for the CCOS dataset were found to contain 2 m sites without explicitly being identified as such. In addition, some of the CCOS observations are hour averaged values, rather than the 5-minute averages used by the NWS. These differences in the observed speeds between the two datasets were the primary reasons why the simulations with observational nudging to the CCOS data produced slower wind speeds that the runs with no nudging or nudging to the NWS data.

The W3O and W4O runs were selected as the " best" runs. The statistical performance was comparable to past runs performed for photochemical modeling purposes. Since the W3O run did not have the low nighttime temperature bias and covered a larger domain with a consistent resolution, this run became our primary focus.

Additional Analyses Specific to the Bay Area

ATMET produced a series of graphics from the W3O run in which the model simulated vector wind fields were displayed with the surface observations. These have been posted to a web site: http://bridge.atmet.org/baaqmd/forecast.php; the web site figures also present a graphical depiction of the statistical results and show the wind speed differences along with wind direction deviations.

Focusing on three days of this episode (30 July through 1 August, 2000), ATMET analyzed RAMS predicted low-level (14.4 m) winds compared to surface mesonet observations at 11 AM and 5 PM local time each day. On 30 July, RAMS simulated winds followed the observed divergent flow pattern over the Bay area, but wind speeds were somewhat low compared to observations. The wind speed through the Golden Gate gap was also low, and the turning of the wind direction due to the sea breeze effect, especially along the west side of the bay, was also underdone. This was likely due to the model grid resolution, which did not fully capture the details of the bay coastline. In other areas, the RAMS forecasts compared reasonably well in wind speed and direction. These general features were also observed in the wind forecasts for 31 July and 1 August. RAMS predictions indicated a general decrease in wind speed through the three-day period, consistent with the observed weakened sea breeze.

A direct comparison of RAMS predicted winds with wind profiler data was conducted by horizontally interpolating the RAMS forecasts to the wind profiler locations; specific analyses were undertaken for the Richmond and Dublin soundings. The predicted morning flow reversal from westerly to easterly and then back to westerly was evident on 31 July and 1 August, and not on 30 July, which compared well with the wind profiler observations. RAMS successfully captured these convergence zones as an above-surface feature, but the lower limit of the flow reversal was predicted down to about 225 meters, while wind profiler observations indicated this level to be somewhat higher at Richmond.

Vertical virtual temperature information was available from several Radio Acoustic Sounder System (RASS) sites within the region of focus. Comparisons of RAMS virtual temperature forecasts with RASS observations are described by ATMET (2004) for Richmond and Dublin. RASS observations indicated a significant morning temperature inversion on 30 July, but much less of an inversion on the mornings of 31 July and 1 August. This suggests the possibility for greater downward vertical mixing of easterly momentum into the marine layer that counteracted the sea breeze flow on these later days, resulting in the Bay Area convergence zone as discussed above.

The RAMS virtual temperature forecasts indicated a small cool bias for most time periods at both locations when compared to RASS observations. The cool bias was greatest during the morning hours when the temperature inversion was significant. It is likely that the model vertical resolution was insufficient to fully capture the inversion. Predictions were much closer to observations during the afternoon hours when the marine layer appeared to be more fully

mixed in the vertical. RAMS predictions indicated the morning inversion on the 30th, and then a weaker morning inversion on the 31st and the 1st. RAMS, however, tended to be less stable in the marine layer during the afternoon hours. This would allow greater downward vertical mixing into the marine layer, and this likely contributed to the lower than observed easterly flow in the marine layer that was noted in the RAMS vs. wind profiler comparison.

One of the interesting features in the wind profiler data was the consistent diurnal wind direction shift above the boundary layer for the two Bay area locations (Richmond and Dublin). The wind direction shifted from a westerly to easterly component around 4 AM local time, and then reversed back to a westerly component around midday. RAMS forecast winds from about 740 m AGL for 31 July indicated this wind direction shift as well. During the early morning hours, predicted flow was northeasterly over much of the region. Later in the morning, 10 AM forecast winds veered toward northerly and even northwesterly over portions of the Central Valley. After midday, the wind shift was apparent with nearly all areas showing a predicted wind direction with some westerly component.

A portion of this mid-day wind shift was likely attributed to the low-level westerly flow mixing upward through time, especially over land areas west of the Coastal Range. It is, however, unlikely that this feature was entirely responsible for the domain-wide gradual wind shift. It is possible that the high Sierra mountain range to the east also influenced this shift where elevated daytime heating can draw flow from the west, and nighttime drainage flow can create a reversed easterly push. West-east vertical cross-sectional analyses of the predicted flow were consistent with this supposition. During the early morning hours (2 AM), the predicted flow showed the generation of easterly drainage flow along the west slope of the Sierra. Model results suggested that with time the drainage flow spread westward above the marine boundary layer and extended to over the Pacific coastal region. A weak easterly component was indicated at 4 AM over the Bay area that was consistent with the wind shift noted in the wind profiler observations. The layer of easterly-component flow became strongest around 7 AM and then gradually eroded with time from the east until the entire flow contained a westerly component by 1 PM, also consistent with the observed mid-day wind shift in the profiler data.

The positioning of the subtropical high to the northwest also likely played a role in this scenario, whereby the absence of the typical on-shore synoptic flow is not able to overwhelm this mountain-valley circulation. One might also speculate that 850 mb easterly synoptic flow could have created enhanced downslope winds off the Sierra, but the cross-sectional forecasts did not indicate any such effect. Whatever the cause of the wind direction shift, it would seem feasible to conclude that the diurnal slosh of air from west to east during the day and then back west at night would allow pollutants from previous days (and from inland fires) to recirculate back over the populated coastal regions. This feature, combined with the strong thermal cap at 850 mb and the greater than usual boundary-layer mixing due to less cloudiness and stronger surface heating, all create a scenario conducive to creating elevated levels of pollutants.

Discussion

Some additional comments can be made based on the subregion results:

- A large majority of the stations showed very good diurnal behavior of the wind speed comparing the RAMS results to the observations;

- As expected, the RAMS wind speeds verified best against the NWS stations, given that the simulated winds are representative of a 30 m deep layer and the NWS observations are taken at 10 m height.
- There were significant differences in the observed late afternoon, peak mean wind speeds when the stations were stratified by station type. For example, for the Bay Area subdomain, the NWS stations had an average mean peak speed of about 6 m/s, the CCOS 10 m+ stations were about 4.5-5 m/s, and the CCOS unmarked stations were about 4-4.5 m/s. The only possible explanations we have at this point, assuming the instruments were calibrated correctly, are that some stations were not correctly identified at the appropriate height level, or that siting differences between the CCOS and NWS sites (typically at airports) are significant enough to cause additional surface drag at sites such as AIRS.
- When looking at the Sacramento subdomain, we saw a better agreement between the peak mean values between the NWS and the CCOS 10 m+ observations (4.5-5 m/s). However, these CCOS stations had peak means much closer to the 2 m stations (2.5-3 m/s). The SJV subdomain had similar results to the Sacramento subdomain.

Why are these differences between the wind speed observations important? There are two aspects: 1) determining how to verify and evaluate the meteorological simulation results, and 2) selecting which observations should be used in the four-dimensional data assimilation (FDDA) procedures of the meteorological models to be scientifically consistent with the schemes.

The FDDA schemes in both RAMS and MM5 use the input surface observations to nudge the near-surface winds (actual effective depth of the nudging is a model input parameter) in an attempt to correct any discrepancies between the model simulation and the observations. However, as we discussed, the lowest layer of the models do not necessarily correspond to the depth for which the surface observations are representative. Therefore, from a scientifically-defensible viewpoint, it is inconsistent to use, for example, a 2 m wind observation to nudge a 30m deep model layer. As discussed in detail at one of the Model Advisory Committee meetings, results from CAMx runs between RAMS and MM5 simulations showed higher ozone amounts in the MM5 run. The primary difference between these runs was that the MM5 run had significantly lower wind speeds, which verified more closely with the lower observed mean peaks from the CCOS dataset, as opposed to the higher peaks of the NWS stations. As presented at the MAC meeting, this is most likely a case of " compensatory errors", where the slow wind speeds will lead to less ventilation of ozone and the precursors, partially compensating for deficiencies in the emission inventories and the low ozone biases reported from the photochemical modeling.

As suggested by the analysis of the observations in ATMET (2004), the representation of convergence zones aloft over the Bay Area is very important. Further, given that the convergence zones in the central California region frequently do not extend to the surface, the use of surface wind observations in an attempt to force larger-scale phenomena that the model may not be suitably configured to replicate becomes even more problematic.

Simulations of July 1999

The RAMS runs for the July 1999 episode followed from the configuration of the July/August 2000 runs, with some features from the June 2000 episode. The Bay temperature was held at the same constant 19°C, as observations from the USGS showed a similar average temperature for July 1999. Some experiments for the June 2000 runs, in which the soil moisture was made higher for elevations over 500 m, showed some promise, so this was used for some simulations for this episode. The analysis nudging also borrowed a modification made for the June 2000 runs, where the analysis nudging was turned off below 3-3.5 km above sea level, allowing the lower atmosphere to adjust more completely to the physiographic forcing and observational nudging. This also allowed a more complete development of the coastal fog and stratus.

The observational nudging used a variety of mesonet datasets provided by CARB. These included CIMIS, RAWS, AIRS, BAAQMD, buoys, and the NWS sites. As in the first episode, only wind observations were used in the observational nudging. All wind observations were used for the nudging, even though a significant number of these were taken from sites with low (<10 m) probe heights. Furthermore, this modeling was undertaken prior to intensive efforts by BAAQMD staff to screen the data and to fix major problems seen in the CARB data compilation for this episode. Numerous stations were excluded from the analysis after ATMET performed their own visual quality-control procedure on the time traces of the meteorological parameters. Several stations had frequent occurrences of too high wind speeds, others had temperature observations that dropped to too low values. There were a few stations that appeared to have consistently too low wind speeds, but they were not removed.

Selection of the Best Configuration

ATMET (2004) reports on a series of nine separate full-episode RAMS simulations; results are summarized here. Three 3-grid runs were performed, and six follow-on 4-grid runs were performed. The 3-grid runs were configured as follows:

- A3: “dry” initial soil moisture content, no nudging of any kind, 19°C bay surface temperature, Harrington short-wave radiation, Chen long-wave radiation;
- B3: “medium” initial soil moisture content (higher moisture on terrain above 500 m MSL), analysis nudging above 3.5 km AGL, 19°C bay surface temperature, Harrington short- and long-wave radiation;
- C3: as in B3, but with higher horizontal diffusion.

These runs showed the difference between no analysis nudging (A3) and the use of the analysis nudging (B3 and C3), in this case where only analysis nudging to the upper air fields was performed. The statistical evaluation of the C3 run was very reasonable for this type of simulation. Very little bias was apparent in the wind speed (mostly < 1 m/s) and dewpoint temperature. There was some warm temperature bias during the first half of the simulation, but by the days of the exceedances (11th and 12th), the bias had all but vanished.

With the good statistical performance of the C3 run, we proceeded to focus on the full 4-grid runs for further testing. The best three 4-grid simulations were:

- C4: "medium" initial soil moisture content, analysis nudging above 3.5 km AGL, 19°C bay surface temperature;
- D4: "medium" initial soil moisture content (higher moisture on terrain above 500 m MSL), analysis nudging above 3.0 km AGL (stronger on grid 4), 19°C bay surface temperature;
- O4: as in C4, but with observation nudging to surface wind observations.

Except for the dewpoint temperature, these three simulations exhibited similar behavior. Statistical comparisons clearly showed that the enhanced soil moisture at higher elevations was beneficial to the simulation. The D4 simulation provided the best overall performance for the 4-grid runs. Because of the soil moisture differences, the effect of the observational nudging in run O4 was inconclusive.

Comparisons of runs C3 and D4 showed that both over predicted wind speed (about 1 m/s) in the late afternoon when comparing the RAMS first layer winds to the mesonet observations. In the case of the July 1999 mesonet data, it is known that there is a significant fraction of wind observations taken at 2 m above the ground. Therefore, it is not surprising that this "over prediction" is seen when comparing the results in this manner. ATMET (2004) notes that when comparing the mean observed late afternoon peaks between the NWS and mesonet data there is a similar magnitude of difference (peaks of 6 m/s versus 3-4 m/s) as there was in the July/August 2000 episode (comparing the NWS observations versus the full CCOS dataset). For further analysis of this episode, we will concentrate on the C3 and D4 runs, again mostly focusing on the 4-km grid of the C3 run.

Additional Analyses Specific to the Bay Area

As with the July/August 2000 episode, for further analysis of the " best" runs for the July 1999 episode, ATMET (2004) focused on the surface wind fields, since they are perhaps the most important meteorological feature for photochemical modeling. We have produced a similar series of graphics from the C3 run in which the model simulated vector wind field is displayed with the observations. These figures are also available from the web site: http://bridge.atmet.org/baaqmd/forecast.php.

Since this episode did not occur in conjunction with a field program, the profiler and RASS data were not available. RAMS predicted low-level (14.4 m) winds were compared to surface mesonet observations for 11 and 12 July at 11 AM and 5 PM local time each day. The key surface feature in the observations was the indication of a convergence zone east of the bay, a feature not evident in the first case. RAMS predicted winds captured the convergence zone quite well at 11 AM on the 11th. At 5 PM, however, it appeared that the model prediction somewhat over predicted the strength and inland penetration of sea breeze, and hence did not indicate the convergence zone in eastern Contra Costa as seen in the mesonet observations. RAMS wind predictions for the 12th were consistent with observations. The well-defined convergence zone at 11 AM matched well with observations. At 5 PM, westerly winds moved over the entire region west of the Coastal Range that again matched well with observations.

The RAMS forecasts for this case show some interesting similarities and differences when compared to the first case. The most notable similarity is the above-boundary-layer diurnal wind

direction shift. Although the details are somewhat different than the first case, the wind direction shifted as in the first case from a westerly to easterly component around 4 AM local time and then reversed back to a westerly component around mid-day. During the early morning hours, predicted flow was easterly over the Carquinez Strait and mostly southeasterly over San Francisco Bay, Alameda County, and the Central valley. The positioning of the subtropical high in this case was such that low-level synoptic flow was easterly as compared to northeasterly in the first case, and this is the likely reason for the wind direction veering by about 45 degrees from the first case. Later in the morning at 10 AM, forecast winds continued from the east and northeast over the Carquinez Strait, while wind directions tended to veer to southerly over the Central Valley. After mid-day, the wind shift was apparent with nearly all areas showing a predicted wind direction with some westerly component.

Similar to the first case, the wind shift is likely the result of two components: 1) the low-level westerly flow forced by sea breeze mixing upward through time over land areas west of the Coastal Range; and 2) the larger scale diurnal mountain/valley circulation created by the high Sierra located to the east. West-east cross-sectional analyses of the predicted flow for the July 1999 case also supported this hypothesis. The easterly drainage flow was stronger in this case, which was likely enhanced by the low-level synoptic easterly flow. The early morning (1 AM) easterly-component flow has already reached the Central Valley floor and has begun to push over top of the marine boundary layer. By 4 AM, the easterly flow has extended over the Pacific Ocean, consistent with the wind shift noted at in the July/August 2000 case. However, the drainage flow had effectively mixed out and removed the marine boundary over the Coastal Range and, at 10 AM had eroded some of the marine boundary layer over the San Francisco Bay area. The mid-day wind direction shift still occurred with westerly-component flow in the lowest 2000 m at 1 PM. At 4 PM, a well developed solenoid flow was evident over the Coastal Range and was likely attributed to upward vertical motion resulting from significant afternoon heating of the elevated terrain. Unlike the first case, mountain wave effects were also apparent.

RAMS-predicted boundary layer flow at 85 m AGL illustrates some interesting differences between the two cases. With the indication of the drainage flow eroding the morning boundary layer over the Coastal Range, northeasterly flow was evident through the Carquinez Strait and west of the Coastal Range at 7 AM. This flow was weakly enhanced by downslope effects as suggested in the previous cross-sectional analyses. The result was low-level convergence through the middle of the San Francisco Bay area. With a significant land/water temperature gradient, a well-developed sea breeze was evident at 10 AM throughout the San Francisco Bay area and westerly flow also pushed through the Carquinez Strait. Wind speeds strengthened across San Francisco Bay through the afternoon. A more detailed cross-sectional analysis of the predicted flow suggested that downslope effects to the lee of the San Francisco peninsula act to enhance the wind speed in this area. This is not surprising given the erosion of the marine boundary layer even over the San Francisco peninsula. With significantly weaker stability, the boundary layer flow was no longer channeled through the Golden Gate Gap but rather flowed freely over top of the elevated terrain.

The overall similarity between the two episodes appears to be tied to the position of the Pacific Basin subtropical high and may indicate that this specific type of meteorological situation must be present for ozone exceedances to occur in the Bay Area. Model results suggest that off-shore synoptic flow above the boundary-layer creates a scenario that allows for the development of a mountain/valley circulation forced by the Sierras. This circulation can advect daytime pollutants out of the San Francisco Bay basin, but then can return them to the coastal regions at night. In

conjunction with other synoptic features including the strengthening of an 850 mb thermal cap and an eroding marine boundary layer that allows for greater sunshine and enhanced vertical mixing, the scenario is set for potentially elevated ozone levels.

The positioning of the subtropical high also created differences in the two episodes. Synoptic flow at 850 mb was northeasterly for the first episode and easterly for the second case. The largest differences were noted in the marine boundary layer. The stronger off-shore synoptic flow in the second case enhanced the drainage flow off the Sierra such that the boundary layer eroded soon after sunrise over the Coastal Range. This setup then created significant flow convergence over San Francisco Bay. Also, enhanced morning heating over the elevated terrain of the Coastal Range created a significant water-land temperature gradient that forces an abnormally strong sea breeze to form across the valley. Valley temperatures remained warm, however, which in turn allowed for enhanced vertical mixing that can transport high ozone air from aloft down to the surface. This effect may have also been enhanced by weak downslope winds that form in the lee of the San Francisco Peninsula where the afternoon marine boundary layer had also eroded.

The same wind observation issues are applicable to the simulations with the July 1999 episode also. For the SFBA subregion, the peak mean wind speed among the NWS stations ranged 5.5-6.5 m/s through the episode. The RAMS simulation of the lowest layer winds again verified well with these stations. However, the BAAQMD mesonet, which is supposed to have the same 10 m height of wind observations, had peak mean speeds of only 3.5-5 m/s. The other mesonets (CIMIS and RAWS) had the expected results of lower peak means, since the wind probes are generally lower (2 m height).

Summary from RAMS Applications

ATMET (2004) presents a brief analysis of the meteorology for the July/August 2000 and the July 1999 ozone exceedances episodes in and near the Bay Area. The observations in these cases, as with numerous other ozone episodes in other locations, indicate that convergence zones are important in focusing ozone and the precursors. The convergence zones in these cases were caused by the interaction of the on-shore sea breeze flow within the marine layer with the easterly large-scale flow forced by the subtropical high. When the winds and temperature allow, the easterly flow can erode the marine layer over the Central Valley and Coastal Range, causing near-surface convergence zones to occur. An important finding in the analysis shows that the convergence zone frequently does not extend to the ground. This finding has significant implications for verification and four-dimensional data assimilation applications.

Overall, the RAMS simulations performed for the July/August 2000 and the July 1999 episodes show verifications that are consistent with past simulations of this type, with errors of especially wind speed and temperature within the range expected. We have pointed out various issues with the input datasets that have been used for the verifications and the four-dimensional data assimilation schemes.

While the error statistics were acceptable for the most part, there were various aspects of the simulations of this region that need to be addressed to make significant improvements in the results:

- Even with the 1 km resolution grid, it is our opinion that higher resolution is still needed to resolve the important topographical features.
- The same higher resolution issue is apparent when considering land use features such as coastlines, wetlands, urban areas, etc.
- With the higher resolution also comes the need for higher resolution datasets of topography and land use, since the datasets used by atmospheric models are usually 30 second (about 1 km) resolution. Much higher resolution datasets do exist, especially for topography.
- There was no information on what areas were in active irrigation during these episodes. There was circumstantial evidence that various areas were active, since stations located very close together in the Central Valley sometimes had very different temperatures and dewpoints.

The complexity of the central California meteorology, with complex terrain and land use features, along with the interactions of marine and mountain flows, poses a difficult situation to simulate with current models. This puts a reliance on the FDDA to introduce large scale changes into the mesoscale domains. But too often, the FDDA also serves the purpose of attempting to correct model errors, sometimes with undesirable results. The situations in these cases point this out very clearly; the vast majority of the observed data used in the FDDA are taken at or very near the surface. However, the primary forcing mechanisms for the important flows may not ever become apparent at the surface. And there were far too few observations taken above the surface, even during CCOS with the profilers and RASS, to adequately resolve the horizontal structure of the meteorology above the marine layer.

There is one other important meteorological modeling implication of the elevated convergence zone. It is imperative in these complex layers of stability that the subgrid scheme employed in the meteorological model be able to correctly treat elevated well-mixed, neutral layers. Many of the models use simple, surface-based PBL schemes that either: 1) produce a single PBL from the surface to some defined PBL height, usually resulting in a too deep boundary layer that mixes out the shallow surface stable layer, or 2) overemphasizes the effect of the surface stable layer and shuts down vertical mixing throughout the PBL. It is necessary to employ a TKE-based scheme that has all of the necessary physical terms (advection, production, diffusion, dissipation) to correctly handle elevated mixed layers and these types of elevated convergence zones.

MM5 APPLICATIONS

Initial MM5 simulations were performed for the CCOS July/August 2000 episode by the CARB and their meteorological modeling contractor at NOAA/ARL, concurrent with the initial ATMET RAMS simulations. Later, the BAAQMD instituted their own internal MM5 modeling effort for the July/August 2000 episode. Subsequent MM5 modeling of the ancillary July 1999 episode was undertaken by both the CARB and BAAQMD.

Description of MM5

The PSU/NCAR MM5 is a state-of-the-science atmosphere model that has proven useful for air quality applications and has been used extensively in past local, state, regional, and national modeling efforts. MM5 has undergone extensive peer-review, with all of its components continually undergoing development and scrutiny by the modeling community. The MM5 modeling system software is freely provided and supported by the Mesoscale Prediction Group in the Mesoscale and Microscale Meteorology Division of NCAR. For these reasons, MM5 is the most widely used public-domain prognostic model. In-depth descriptions of MM5 can be found in Dudhia (1993) and Grell et al. (1994), and at http://www.mmm.ucar.edu/mm5.

The MM5 is a limited-area, terrain-following (sigma-coordinate), prognostic meteorological model. It solves the full suite of non-hydrostatic prognostic primitive equations for the three-dimensional wind, temperature, water (in all phases), and pressure fields. It can be run with multiple one-way or two-way nested grids to resolve a range of atmospheric processes and circulations on spatial scales ranging from one to several thousands of kilometers. The model is highly modular, facilitating the interchange of physics and data assimilation options. Several options exist for boundary layer schemes; resolved and sub-grid cloud and precipitation treatments; soil heat budget models, and radiative transfer. The model equations are solved horizontally on an Arakawa-B grid structure defined on a number of available map projections. The Lambert conformal conic projection is used for air quality applications in the U.S. The vertical coordinate is a terrain-following normalized pressure coordinate, referred to as a "sigma-p". Typically, 30-50 vertical levels are used to resolve the troposphere and lower stratosphere to ~15 km.

The model is supported by several pre- and post-processing programs, which are referred to collectively as the MM5 modeling system. The MM5 modeling system software is mostly written in Fortran, and has been developed at Penn State and NCAR as a community mesoscale model with contributions from users worldwide. The pre- and post-processing tools facilitate the development of various model inputs, and the analysis of model output.

Because MM5 is a limited-area model, it requires lateral boundary conditions that define the space- and time-varying conditions at the periphery of the coarsest domain throughout the simulation. Both initial and boundary conditions are generally specified using observational analyses, and may be supplemented by additional surface or upper air observations. These data sources can be obtained from a variety of routine analysis systems, from several global analysis products to higher resolution (time and space) forecast initialization fields prepared by the National Weather Service or other entities. Most datasets are available directly from NCAR.

The model may be constrained during the simulation to relax toward observed temperature, wind and humidity observations through the use of four dimensional data assimilation, known as FDDA (Stauffer and Seaman 1990, 1994). FDDA amounts to adding an additional term to the prognostic equations that serves to "nudge" the model solution toward objective analysis fields and/or individual observations. This has been shown to significantly reduce drift in the solution for simulations of several days or more. Drift may be caused by (among other effects) inaccuracies in the initial conditions, the effects of discretization, or errors in the formulation of various parameterizations.

Considerations for Evaluating MM5 Performance

The RAMS meteorological model performance evaluation documented by ATMET (2004) raised significant concerns about the quality and mix of surface observation data compiled into the CCOS meteorological database. In response, ENVIRON undertook a review and compilation of the CCOS surface meteorological measurement data and provided a sub-set of "standardized" observations throughout the state (Emery and Tai, 2004a). The approach entailed identifying and extracting only those sites providing 10 m winds and 2 m temperature for the purposes of standardizing the meteorological performance evaluation among the various groups performing MM5 simulations for CCOS. A revised meteorological dataset for the period spanning July 29 – August 2, 2000 were compiled.

Emery and Tai (2004a) describe the rationale for this activity and the components of the final dataset. They also discuss the concepts that have been adopted among air quality modelers across the U.S. for a rigorous meteorological performance evaluation approach, and describe a set of statistical measures that should be developed and reported relative to "benchmarks" for acceptable performance. Finally, they describe a program that can be used to easily calculate and graphically present these measures on hourly and daily time scales. These topics are summarized below.

The CCOS Meteorological Evaluation Dataset

The CCOS meteorological database includes measurement data taken during the summer of 2000 throughout central and northern California. Data from both existing routine networks and special study sites were collected at the surface and aloft, and are currently managed by the CARB. The BAAQMD undertook an extensive review of these data, identifying and fixing several problems. In further reviewing the CCOS surface meteorological dataset, we identified several issues that impact the quality and consistency of wind, temperature, and humidity measurements, which would therefore obfuscate our quantitative evaluation of MM5 performance. The key issues revolve around: (1) the various probe heights used among and within the various networks; (2) the maintenance status of certain networks (i.e., time since calibration, system checks, etc.); and (3) the lack of data population for the list of sites compiled for the CCOS meteorological database.

Identifying sites by network in the CCOS dataset was difficult. We obtained a site list lookup table/description from the CARB, but meta data did not consistently contain all needed information to fully describe the sites, their mast heights, type of probes, the network to which they belong, etc. Once we began to extract meteorological measurements from the CCOS

database, we found that it is missing all NWS data and all RAWS data (except for one site). ATMET provided hourly NWS data for the July/August 2000 and July 1999 episodes.

For reasons discussed by Emery and Tai (2004a), we removed RAWS and CIMIS stations from inclusion into the MM5 evaluation dataset. Seven sites are located outside the domain in Southern California, and were removed. We included those CARB/District and other miscellaneous sites that explicitly meet the criteria for 10 m winds and 2 m temperature, as determined by information available in the CCOS station meta files or site names. If probe height information was missing for a given site, we assumed a 10 m wind mast and retained the wind observations (Saffet Tanrikulu, personal communication), but disregarded temperature and humidity observations from consideration. Most of these unlabelled sites were from the air quality districts. We also included all data from NWS stations.

The resulting MM5 evaluation dataset includes 242 sites. The data were stratified into the eight meteorological analysis regions shown in Figure 4-4. The data were formatted into the RAMS RALPH v2 format, which is one of two allowable input formats for ENVIRON's METSTAT software. METSTAT also reads observation data in the MM5 binary FDDA format. We chose the RALPH format as it readable ASCII text and is relatively self-documenting. The evaluation dataset was made available on the ENVIRON FTP site (see Emery and Tai, 2004a). Similar procedures were applied to the July 1999 dataset after extensive quality assurance and re-processing by the BAAQMD.

Performance Evaluation Methodology

The goal of the MM5 model evaluation should be to (a) assess whether and to what extent confidence may be placed in the modeling system to provide three-dimensional wind, temperature, moisture, and turbulent mixing rates to air quality models, and (b) compare and contrast performance against results obtained from previous meteorological model applications across the country. The basis for the assessment is a comparison of the predicted meteorological fields to available surface and aloft data collected by the National Weather Service and other reporting agencies. This is carried out both graphically and statistically. A specific set of statistics has been identified for use in establishing benchmarks for acceptable model performance, with the idea that these benchmarks, similar to current EPA guidance criteria for air quality model performance, allow for a consistent comparison of various meteorological simulations for important variables at the surface and in the boundary layer. An extensive summary of the philosophy of model evaluation is provided by Emery and Tai (2004a), based on Tesche (1994) and Tesche et al. (2001).

The focus of this performance evaluation centers on performance in the 4-km grid. However, a regional qualitative analysis should also be carried out in the 36- and 12-km MM5 domains. The first step in the operational evaluation is the preparation of graphics to display the predicted meteorological fields at the surface and for selected levels aloft. This allows for a qualitative assessment of model performance by comparing results to commonly available analysis maps of wind, temperature, pressure, and precipitation patterns available from several entities, including the NWS and others (e.g., http://weather.unisys.com). The purpose of these evaluations is to establish a first-order acceptance/rejection of the simulation in adequately replicating the gross weather phenomena in the region of interest. Thus, this approach screens for obvious model

flaws and errors. Specifically, wind profiler measurements in California provide a very good time-resolved source of data in the vertical, and are used to compare to MM5 output.

Statistical Evaluation

Several statistical measures are calculated as part of the meteorological model evaluation. Additional plots and graphs are used to present these statistics on both hourly and daily time frames. These measures are calculated for wind speed, wind direction, temperature, and humidity at the surface.

The problem with evaluating statistics is that the more data pairings that are summarized in a given metric, the better the statistics generally look, and so calculating a single set of statistics for a very large area (e.g., the entire 4-km domain) would not yield significant insight into performance. Therefore, the statistical analysis is refined to sub-regions within the large grid. Results from the sub-regional evaluations give clues as to any necessary modifications to be made in the MM5 configuration.

Below we list the various statistical measures that should be identified in the study protocol (full descriptions are provided by Emery and Tai, 2004a):

- Mean Observation
- Mean Prediction
- Least Square Regression
- Bias (signed error)
- Gross Error (absolute or unsigned error)
- Root Mean Square Error (RMSE, and systematic/unsystematic components)
- Index of Agreement (IOA)

ENVIRON has derived and proposed a set of daily performance "benchmarks" for typical meteorological model performance (Emery et al., 2001). These standards were based upon the evaluation of a variety of about 30 MM5 and RAMS air quality applications in the last few years, as reported by Tesche et al. (2001). The purpose of these benchmarks was not necessarily to give a passing or failing grade to any one particular meteorological model application, but rather to put its results into the proper context. The key to the benchmarks is to understand how poor or good the results are relative to the universe of other model applications run for California and other areas of the U.S. Certainly, an important criticism of the EPA guidance statistics for acceptable photochemical performance is that they are relied upon much too heavily to establish an acceptable (to the EPA) model simulation of a given area and episode. Often lost in the statistical evaluation is the need to critically evaluate all aspects of the model via diagnostic and process-oriented approaches. The same must stressed for the meteorological performance evaluation.

Emery et al. (2001) carefully considered the appropriateness and adequacy of the proposed benchmarks based upon the results of MM5 simulations performed and reported in that study. Based upon these considerations, the final daily proposed benchmarks are given below:

Wind Speed	RMSE:	≤ 2 m/s
	Bias:	≤ ±0.5 m/s
	IOA:	≥ 0.6
Wind Direction	Gross Error:	≤ 30 deg
	Bias:	≤ ±10 deg
Temperature	Gross Error:	≤ 2 K
	Bias:	≤ ±0.5 K
	IOA	≥ 0.8
Humidity	Gross Error:	≤ 2 g/kg
	Bias:	≤ ±1 g/kg
	IOA:	≥ 0.6

The METSTAT Program

A statistical analysis software package has been developed to calculate and graphically present the statistics described above. The package is comprised of a single Fortran program (METSTAT) to generate observation-prediction pairings and to calculate the statistics, and a Microsoft Excel macro (METSTAT.XLS) that plots the results. Both of these are described by Emery and Tai (2004a).

The program spatially and temporally pairs MM5 predictions with observations for a user-defined time and space window. Only surface-level data are used for the statistical calculations. Since the surface layer in MM5 is usually rather thick relative to the heights at which the observational data were recorded, the METSTAT program includes a micro-meteorological module that scales mid-layer predicted winds to 10 m heights, and mid-layer predicted temperatures to 2 m heights, using common stability-dependent similarity relationships. The program then proceeds to calculate the statistics described above for each hour and for each day of the time window. The following parameters are determined:

- Wind Speed, Temperature, Humidity:
  - Mean Observed
  - Mean Predicted
  - Bias
  - Gross Error
  - RMSE
  - $RMSE_S$
  - $RMSE_U$
  - IOA

- Wind Direction
  - Mean Observed
  - Mean Predicted
  - Bias
  - Gross Error

The RMSE and IOA have not been typically used to quantify error for wind direction, and thus are not calculated by the program.

MM5 Simulations of the CCOS 2000 Period

The meteorological phenomena in the central California region that are known to have a pronounced impact on ozone concentrations include: 1) the sea-breeze, which can bring cooler, moister, and less polluted air as it propagates inland; 2) flow through the San Francisco Bay area, which is the principal inflow to the Central Valley, and the split of this flow, which determines the relative inflow into the Sacramento and San Joaquin Valleys; 3) nocturnal low-level jets, which can rapidly transport boundary layer pollutants along the Central Valley; 4) mesoscale eddies (the Schultz, Fresno, and Bakersfield), which can recirculate ozone and its precursors; and 5) slope flows, which result in transport in or out of the valleys, support boundary layer venting along mountain crests, and produce subsidence or ascending motion over the valleys. In addition, the depth of the atmospheric boundary layer is of critical importance for air quality, as it determines the depth through which pollutants are vertically mixed. To better understand the role of the above meteorological phenomena on ozone transport and mixing, the BAAQMD employed the MM5 meteorological model.

Observational Data

The observational data sets used for the meteorological comparison include 297 surface meteorological stations, 120 surface ozone monitors and network of 25 915 MHz wind profilers. The network of wind profilers (see http://www.etl.noaa.gov/programs/modeling/ccos/data for the site locations) was one of the core sets of meteorological instrumentation used for CCOS 2000. The wind profilers provided hourly averages of wind speed and direction, typically to heights of 3000 m AGL. In addition to winds, the vertical profiles of virtual temperature were measured using the Radio Acoustic Sounding System (RASS) technique, which typically reached heights of 1000 m AGL. The depth of the daytime, convective ABL was also determined from the wind profiler measurements by visually inspecting values of range-corrected signal to noise ratio, vertical velocity (which is large within the convective ABL), and radar spectral width (which is a measure of turbulence intensity) (White, 1993; Angevine et al., 1994; Bianco and Wilczak, 2002).

Model Description and Case Study Characterization

The high ozone episode discussed in this paper occurred from 30 July to 02 August, 2000. During this period, the synoptic meteorology was characterized by a ridge at 500 mb that started to regress toward the west from New Mexico and strengthened on July 27. During the Intensive Operational Period (IOP) of July 30 -August 2, the ridge remained strong and continued to slowly regress toward the west so that by July 31 it was centered near Reno, Nevada. The 850 mb temperature at Oakland reached as high as 27°C and the 500 mb height peaked at 5,970 m. At the surface, high pressure was present over the Great Basin area with its center located to the northeast of the San Joaquin Valley, rendering a weak offshore pressure gradient between San Francisco and Reno and a weak north-to-south gradient from San Francisco to Las Vegas. Under

such a synoptic pattern, the low-level winds were weak and the sky was mostly cloud free over the San Joaquin Valley, a condition conducive to high ozone events.

MM5 simulations for this episode were run using a 36-12-4 km one-way nested model domain. The model domain had 50 vertical stretched levels among which 30 were within the lowest 2 km and the lowest model level was at about 12 m above the surface. The 4 km domain encompasses the CCOS field study area, which extends from the Pacific Ocean in the west to the Sierra Nevada in the east, and from Redding, CA, in the north to the Mojave Desert in the south. Boundary and initial conditions were prescribed using the 6-hourly 40 km NCEP Eta analysis. The simulations began at 12 UTC 29 July, and were run for 120 h, ending at 12 UTC 3 August 2000.

Various MM5 simulations were run testing different combinations of surface and boundary layer parameterizations and land surface models. Comparing these simulations with observations indicates that the most overall accurate simulation was produced when using the Eta planetary boundary layer and surface layer schemes, and the NOAH land surface model (LSM). In addition, this simulation used the Reisner microphysics parameterization, and the Dudhia short-wave and RRTM long-wave radiation parameterizations. The Grell convective parameterization scheme was used on the 36 and 12 km grids. No convective parameterization scheme was used on the 4 km grid. We will refer to this simulation as Run 1.

It is a common practice in air quality modeling for SIPs to assimilate observations into the meteorological model using the nudging FDDA technique in order to obtain the most realistic meteorological forcing of the photochemical model. Thus, a second MM5 simulation was run differently than Run 1, in that it used analysis nudging on the 36 km domain and observational nudging of the profiler and surface winds on the 4 km domain. We will refer to this run as Run 2. In this FDAA run, a nudging term is added to the prognostic equations of wind and temperature, such that the model state is gradually "nudged" toward the observations based on the difference between the two (see, e.g., Stauffer and Seaman, 1994).

In order to illustrate the impact that the LSM and FDDA have on the accuracy of the model simulation, we include in the study a run (Run 3) that is the same as Run 1 except a simple 5-layer soil model was used instead of the LSM.

Results of Comparison

Direct comparisons between the observations and the model output at the observational sites are presented. Because the highest ozone concentration within the San Francisco Bay Area during this 5 day episode occurred on 31 July (Julian Day 213), and the photochemistry for this day is examined in detail in Section 7 of this report, we focus on the direct meteorological evaluation on this day. In addition, we limit our surface observation comparisons to the San Joaquin Valley and the San Francisco Bay Area, and the wind profiler comparisons to profilers located in Richmond (in the San Francisco Bay Area), Sacramento, and Bakersfield, because these are the areas that have ozone violations during this IOP.

Figure 4-5 shows 24-hour time-height cross-sections of winds and virtual temperature from the wind profiler and RASS at Richmond, and the corresponding output from Run 1 and Run 2. It can be seen that during the entire 24-hour period, the simulated winds from Run 1 and the observed winds show a similar transition from westerly to northerly to northeasterly and back to westerly at 500 m AGL. However, there are noticeable differences between the simulated and the observed winds. From 0000 UTC to 0500 UTC, the observed winds are more northwesterly than the simulated winds in Run 1. From 1400 UTC to 1900 UTC the observations show northwesterly winds within the lowest few hundred meters. The simulated winds in Run 1 do not have this northwesterly flow during this time. Similar to Run 1, Run 2 captures the general transition of the winds throughout this 24-hour period. However, from 0000 UTC to 500 UTC, the simulated winds in Run 2 are more northwesterly than in Run1, which is in better agreement with the observations than Run 1. Additionally, in Run 2 the northwesterly flow between 1400 and 1900 UTC is better simulated than in Run 1. Despite the overall positive impact of FDDA, the observed northeasterly flow between 1600 UTC and 2000 UTC between 0.3 km and 1.5 km is better simulated by Run 1 than Run 2. When compared with the RASS data, both Run 1 and Run 2 appear to be colder during the entire 24-hour period than the observations, but Run2 is generally warmer than Run 1, indicating the impact of FDDA of the observed winds on the simulated temperature.

Figure 4-6 is the same as Figure 4-5, except for the Sacramento site. It can be seen that the simulated winds from Run 1 show a persistent westerly flow below 0.25 km through the entire 24-hour period, but in the observations the westerly winds shift to north/northeasterly at 0700 UTC, and shift back to westerly at 1800 UTC. The winds from Run 2 are also persistent westerly in the lowest 0.25 km, but the depth and the intensity of the westerly flow is weaker in Run 2 than Run 1 from 0700 UTC to 1800 UTC. This indicates the positive impact of FDDA because the observations show weaker winds than what were simulated in Run 1. It is interesting that at this site, FDDA of the observed winds not only improved the simulated winds, but also improved the simulated virtual temperature, except near the surface during the night.

At the Bakersfield wind profiler site (Figure 4-7), the simulated winds from Run 1 show a significant difference at lower levels (below 0.5 km) than the observed from 0400 UTC to 1800 UTC. The simulated winds are southerly and much stronger than observed. The simulated winds from Run 2 are in much better agreement with the observations than Run 1 due to the positive impact of FDDA. The simulated temperature from Run 1 is slightly cooler than the observed, while the temperature from Run 2 is warmer than Run 1, especially during the nighttime hours, due to the impact of FDDA of the observed winds.

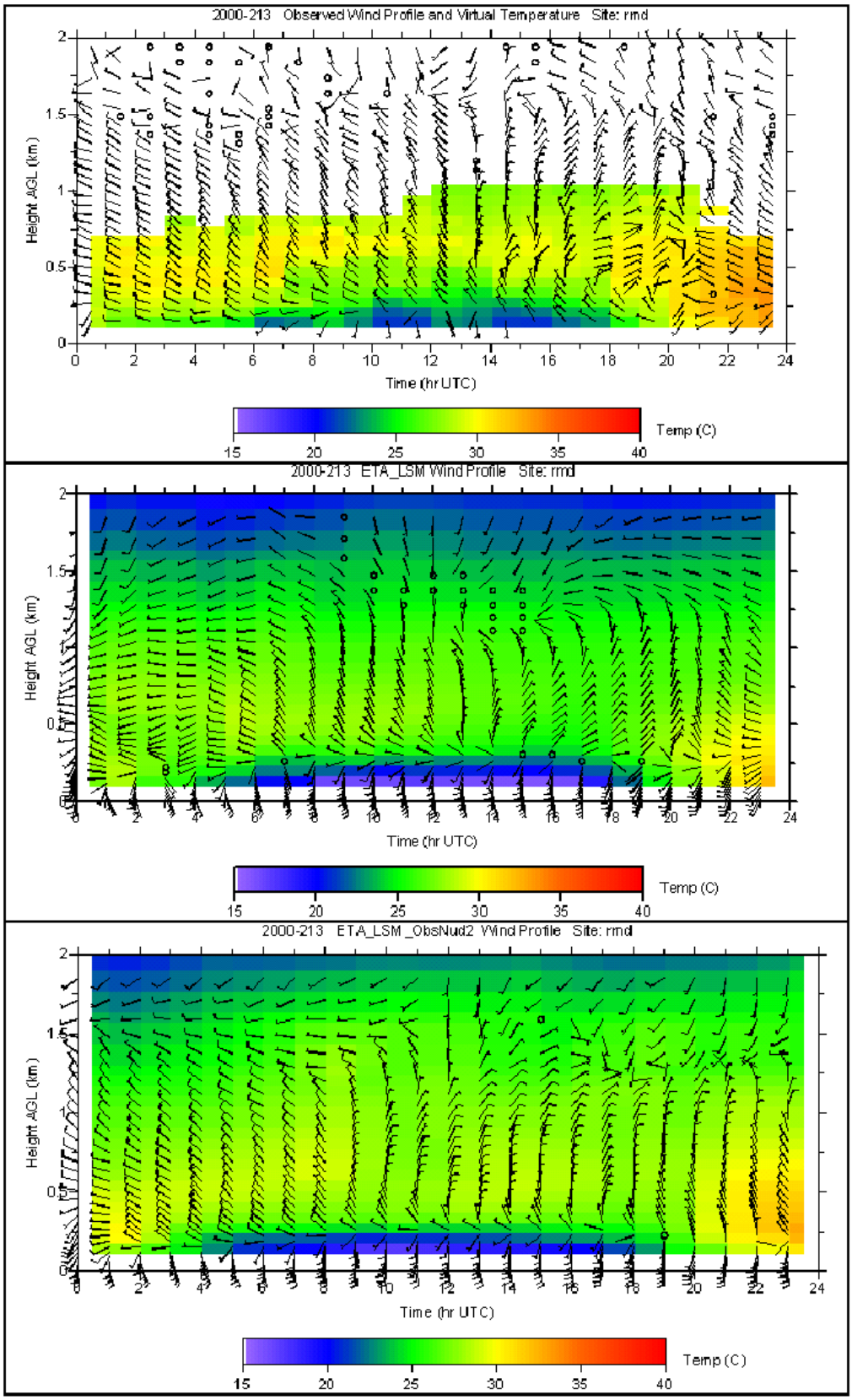

Figure 4-5. Time-height cross-sections of virtual temperature (°C) and winds at the Richmond profiler site on JD 213. Top panel shows the observations, middle panel Run 1, and bottom panel Run 2.

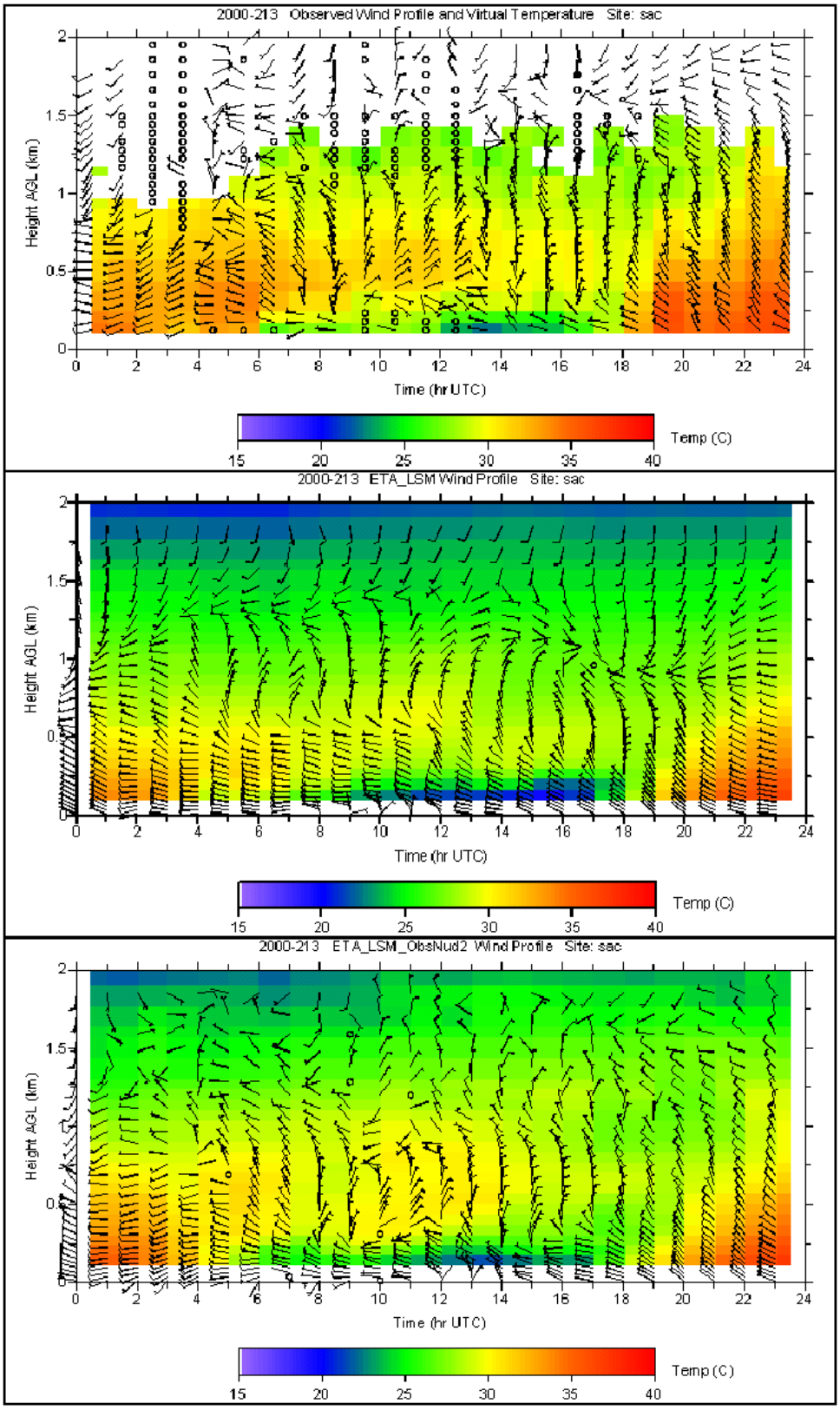

Figure 4-6. Time-height cross-sections of virtual temperature (°C) and winds at the Sacramento profiler site on JD 213. Top panel shows the observations, middle panel Run 1, and bottom panel Run 2.

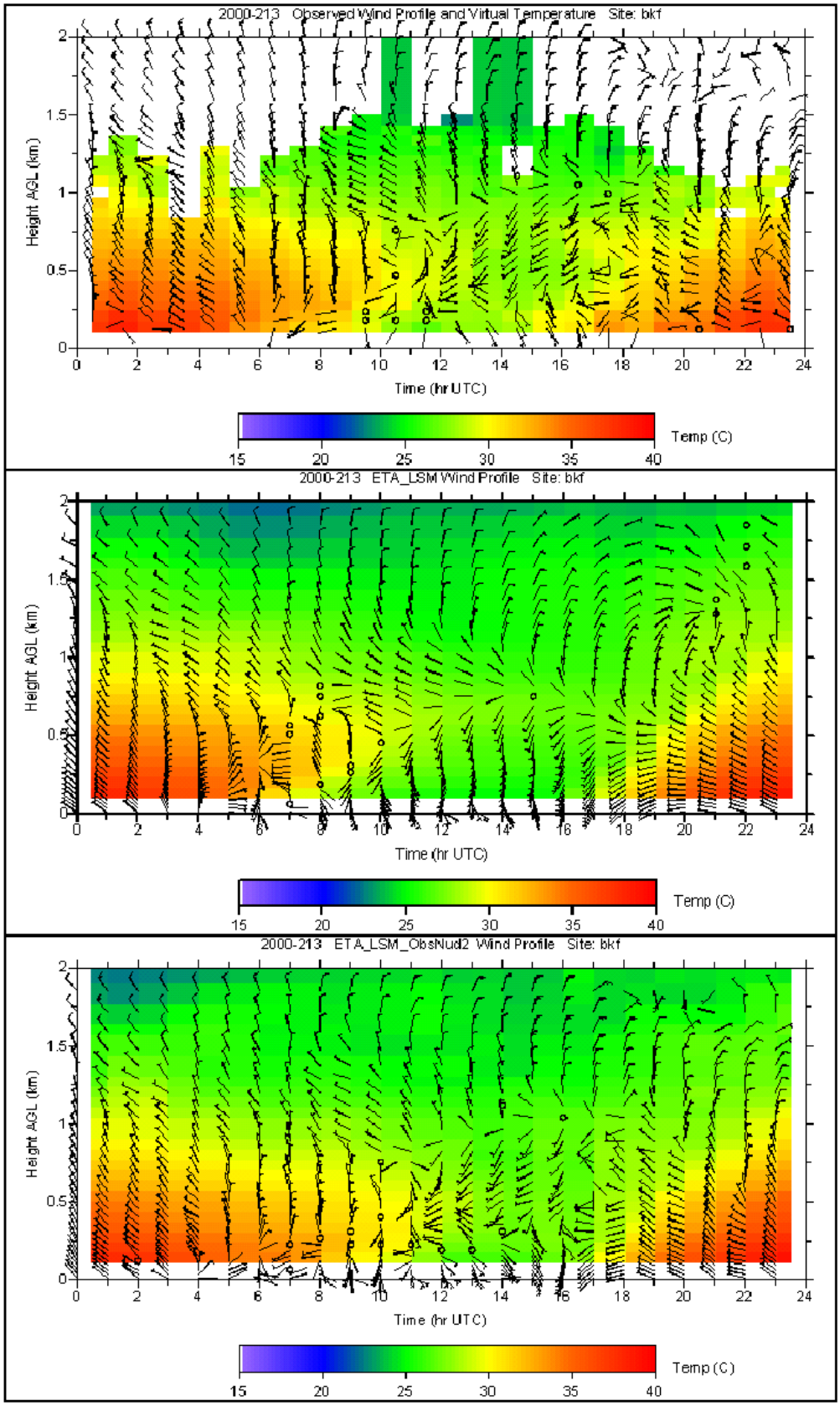

Figure 4-7. Time-height cross-sections of virtual temperature (°C) and winds at the Bakersfield profiler site on JD 213. Top panel shows the observations, middle panel Run 1, and bottom panel Run 2.

Figures 4-8 through 4-11 show the areal average, time series plots of the direction and speed of the observed surface winds as well as the observed surface temperature and dew-point temperature, along with the simulated counterparts from Run 1 and Run 2. The areal average was performed over the San Francisco Bay Area (area 3), and the northern (area 5), the central (area 6) and the southern (area 7) San Joaquin Valley (see Figure 4-4 for the definition of the analysis zones). The mean and absolute biases are given for each area along with the standard deviation. In the wind comparison, we compare wind speed as well as wind direction because the latter is perhaps the most important meteorological parameter for air quality prediction, as it determines the trajectory of pollutant plumes emanating from urban areas or point sources.

The mean and absolute biases vary from one area to another. In the San Francisco Bay area (Figure 4-8), the winds from Run 1 show a similar diurnal cycle as was observed, but with significant discrepancies in wind speed and direction, in particular during the last 3 days of the simulation period. FDDA of the observed winds not only improved both wind speed and direction, but also had an overall positive impact on the surface temperature and dew-point temperature. In the three areas of the San Joaquin Valley (areas 5, 6 and 7), the errors in the winds from Run 1 (Figures 4-9 through 4-11) are greater than those in the San Francisco Bay Area, and it is expected that FDDA would have more impact in these three areas than the San Francisco Bay Area. Indeed, FDDA significantly improved the wind speed and direction as indicated by the time-series comparison and the numbers of the mean and absolute biases corresponding to Run 1 and Run 2. However, although FDDA improved the simulated surface temperature and dew-point temperature from Run 2 in area 5, the mean and absolute biases indicate that it made the simulation of the surface temperature and dewpoint temperature slightly worse in both areas 6 and 7 than Run 1.

From comparisons of the results of Run 1 and Run 2 with the observations, it is clear that the FDDA of the observed winds has a significant, overall positive impact on the simulation of both wind and temperature. To shed light on the impact that the LSM has on the accuracy of the model simulation relative to FDDA, Run1 and Run 3 are compared to the observations. Figures 4-12 through 4-15 show the same areal comparison as the previous four figures, except for the comparisons of Run 1 and Run 3 with the observations. By examining the mean and absolute biases of Run 1 and Run 3 with the observations, it is obvious that although the use of the LSM generally improved the surface temperature and moisture, it increased the biases in both the wind speed and wind direction. This result is important because it indicates that the simple 5-layer soil model was not sufficient to accurately simulate the surface temperature and moisture. Although the use of the more realistic LSM significantly improved the surface temperature and moisture, the wind simulation was somewhat degraded by using the LSM in terms of the mean and absolute biases. Therefore, in order to improve the wind simulation when using the LSM, FDDA of the observed winds was required.

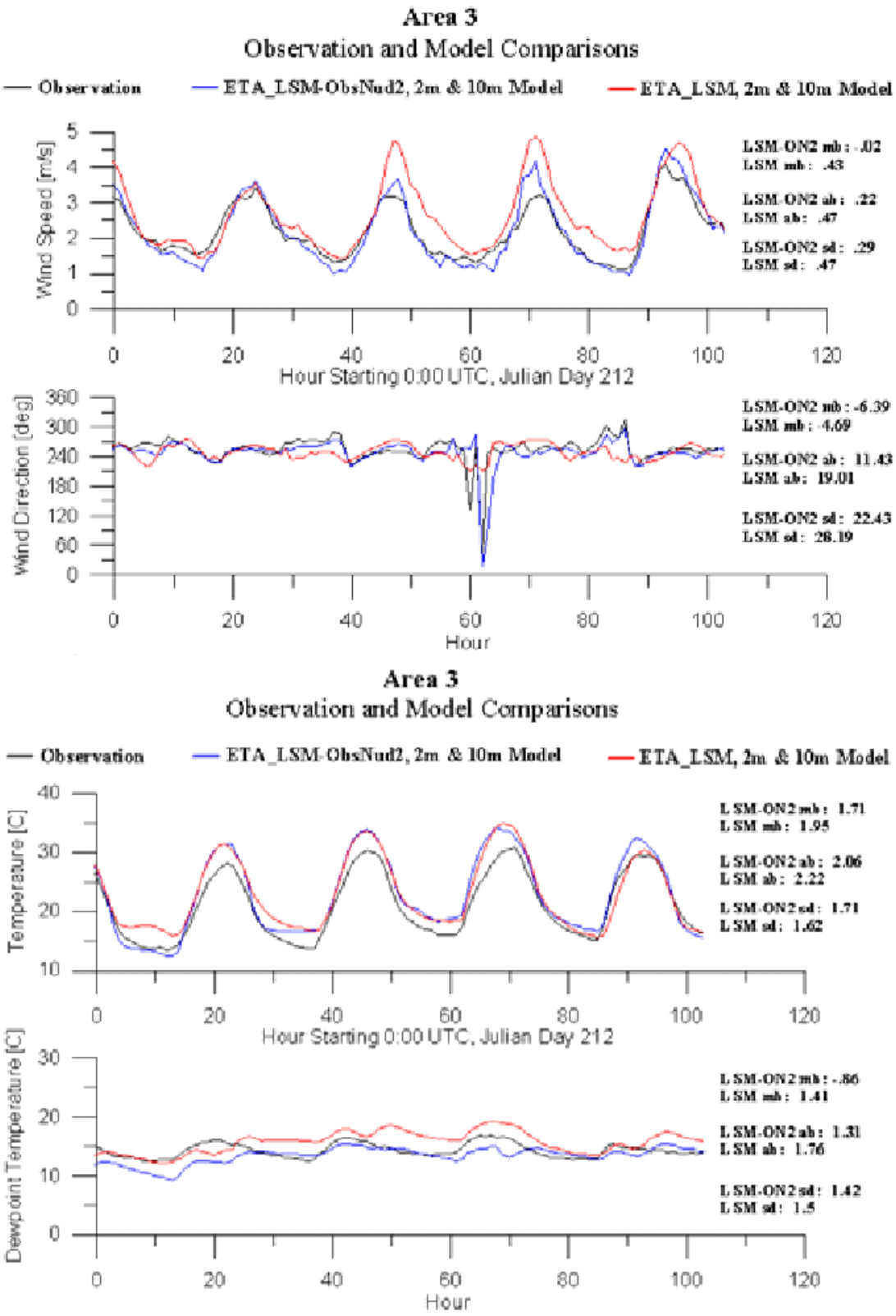

Figure 4-8. Time series of the Area 3 (San Francisco Bay area) average surface meteorology that are arranged from the top panel down: 10-m wind speed (ms-1); 10-m wind direction; 2-m temperature (°C); and 2 m dewpoint temperature (°C). Black line is the observed average, red line is the Run1 average and the blue line is the Run 2 average.

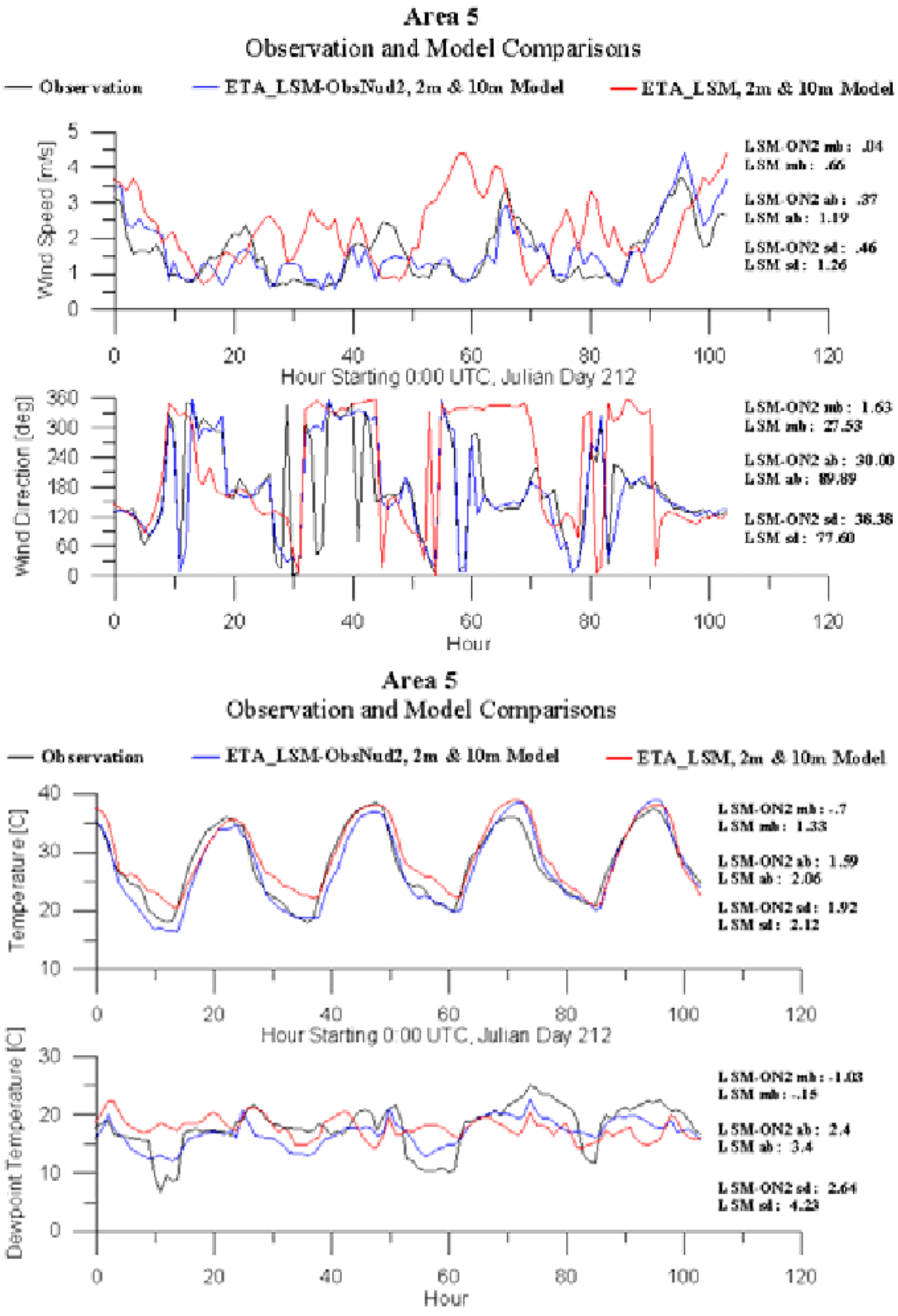

Figure 4-9. Time series of the Area 5 (the northern San Joaquin Valley) average surface meteorology that are arranged from the top panel down: 10-m wind speed (ms-1); 10-m wind direction; 2-m temperature (°C); and 2 m dewpoint temperature (°C). Black line is the observed average, red line is the Run1 average and the blue line is the Run 2 average.

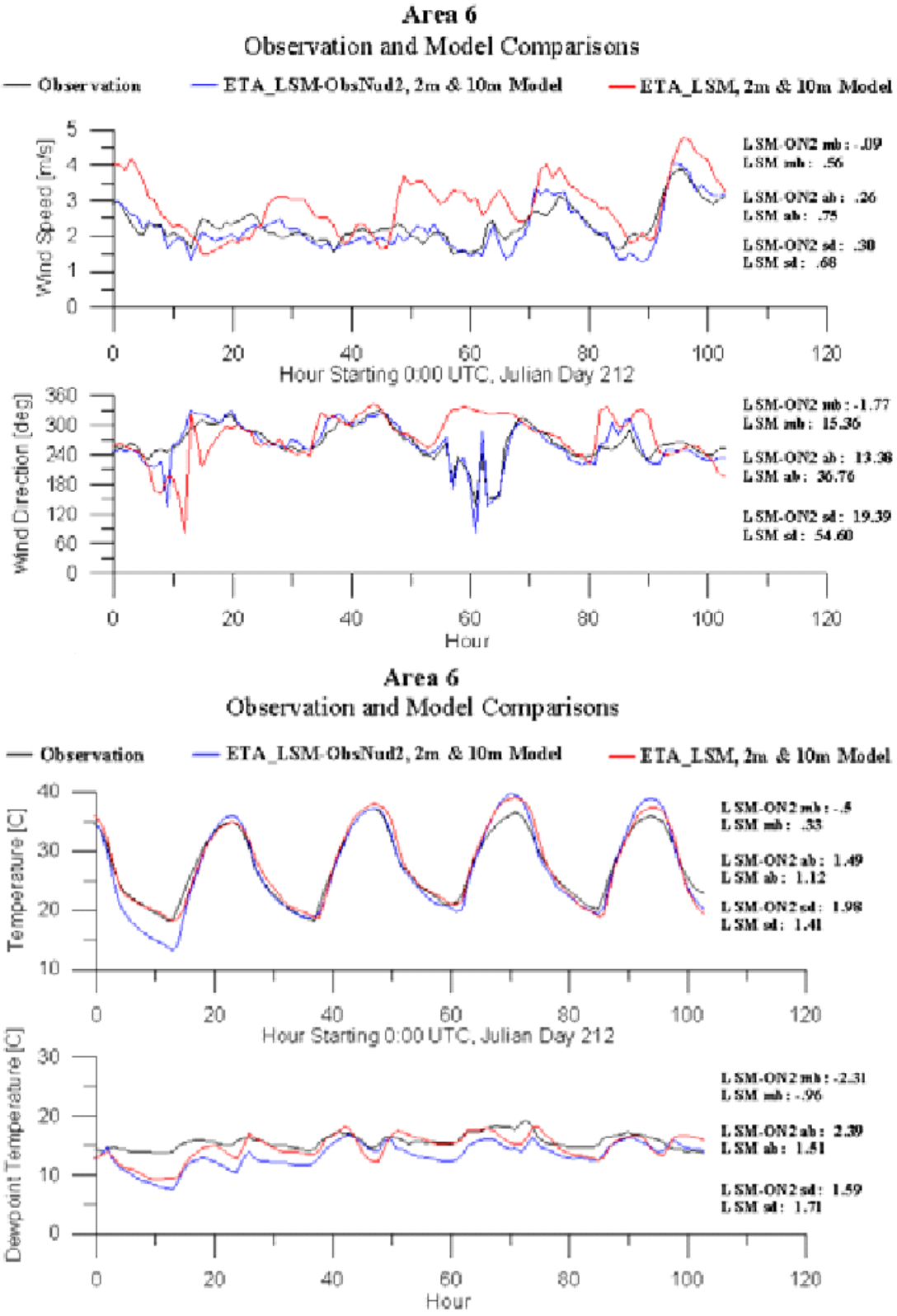

Figure 4-10. Time series of the Area 6 (the central San Joaquin Valley) average surface meteorology that are arranged from the top panel down: 10-m wind speed (ms-1); 10-m wind direction; 2-m temperature (°C); and 2 m dewpoint temperature (°C). Black line is the observed average, red line is the Run1 average and the blue line is the Run 2 average.

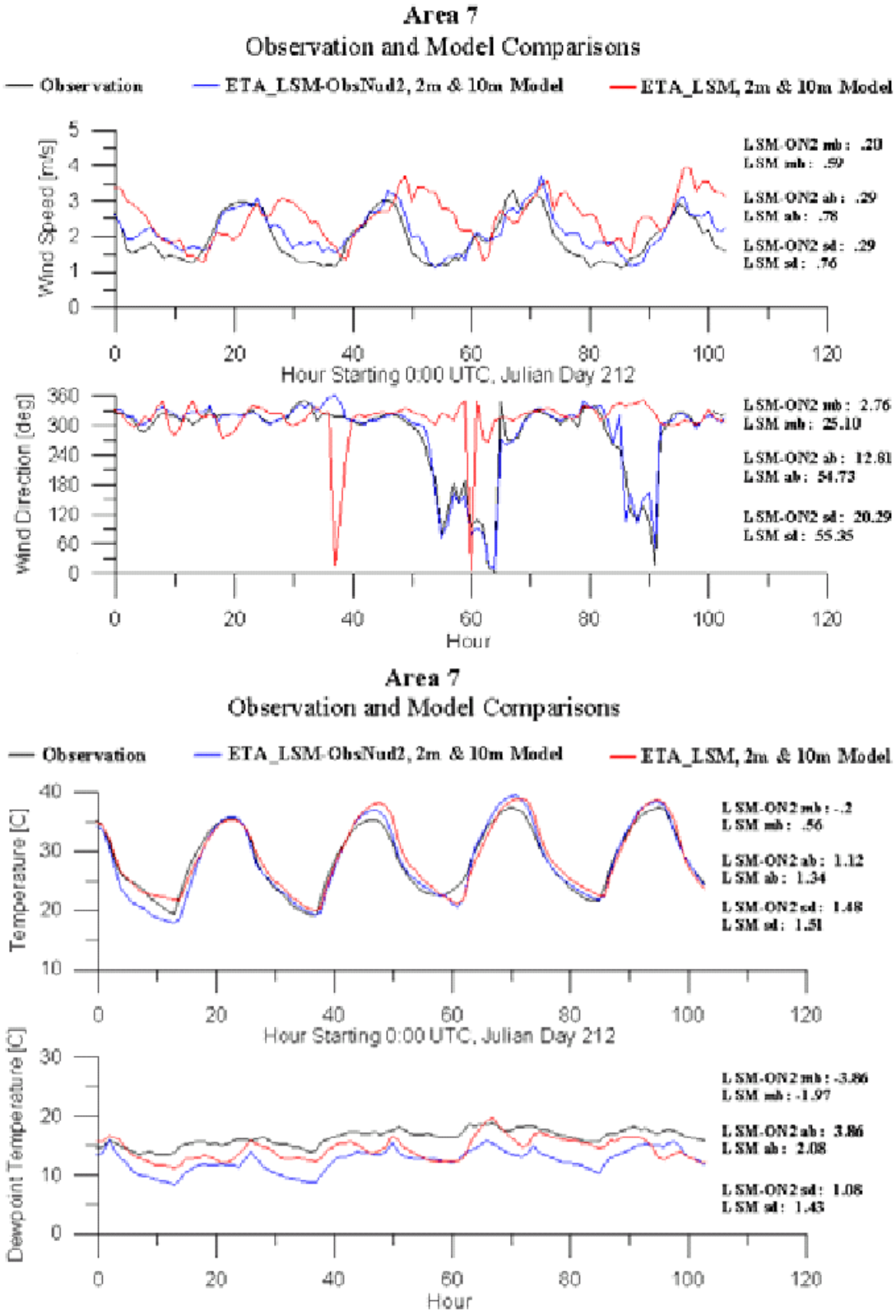

Figure 4-11. Time series of the Area 7 (the southern San Joaquin Valley) average surface meteorology that are arranged from the top panel down: 10-m wind speed (ms-1); 10-m wind direction; 2-m temperature (°C); and 2 m dewpoint temperature (°C). Black line is the observed average, red line is the Run1 average and the blue line is the Run 2 average.

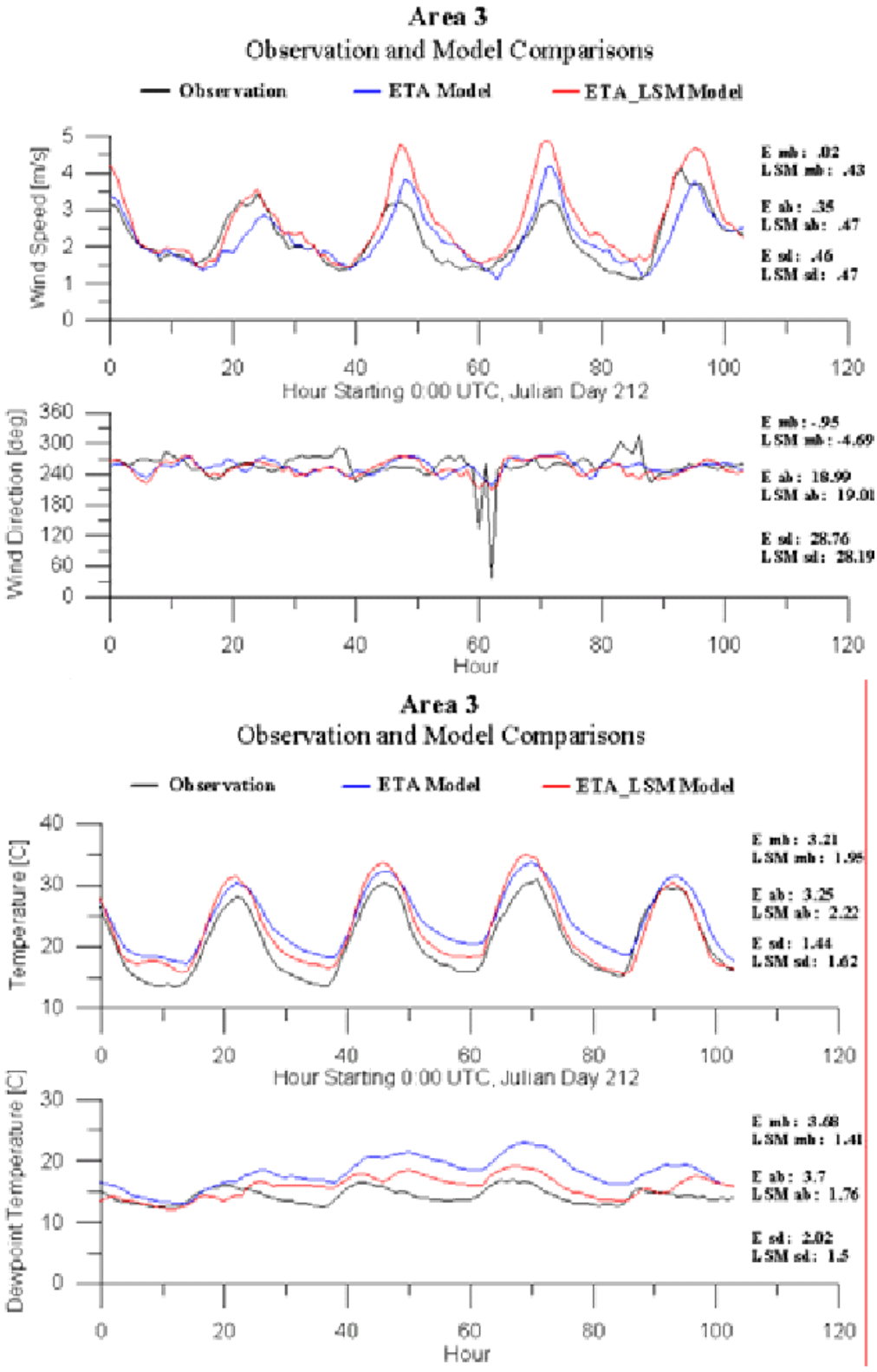

Figure 4-12. Time series of the Area 3 (the San Francisco Bay Area) average surface meteorology that are arranged from the top panel down: 10-m wind speed (ms-1); 10-m wind direction; 2-m temperature (°C); and 2 m dewpoint temperature (°C). Black line is the observed average, red line is the Run1 average and the blue line is the Run 3 average.

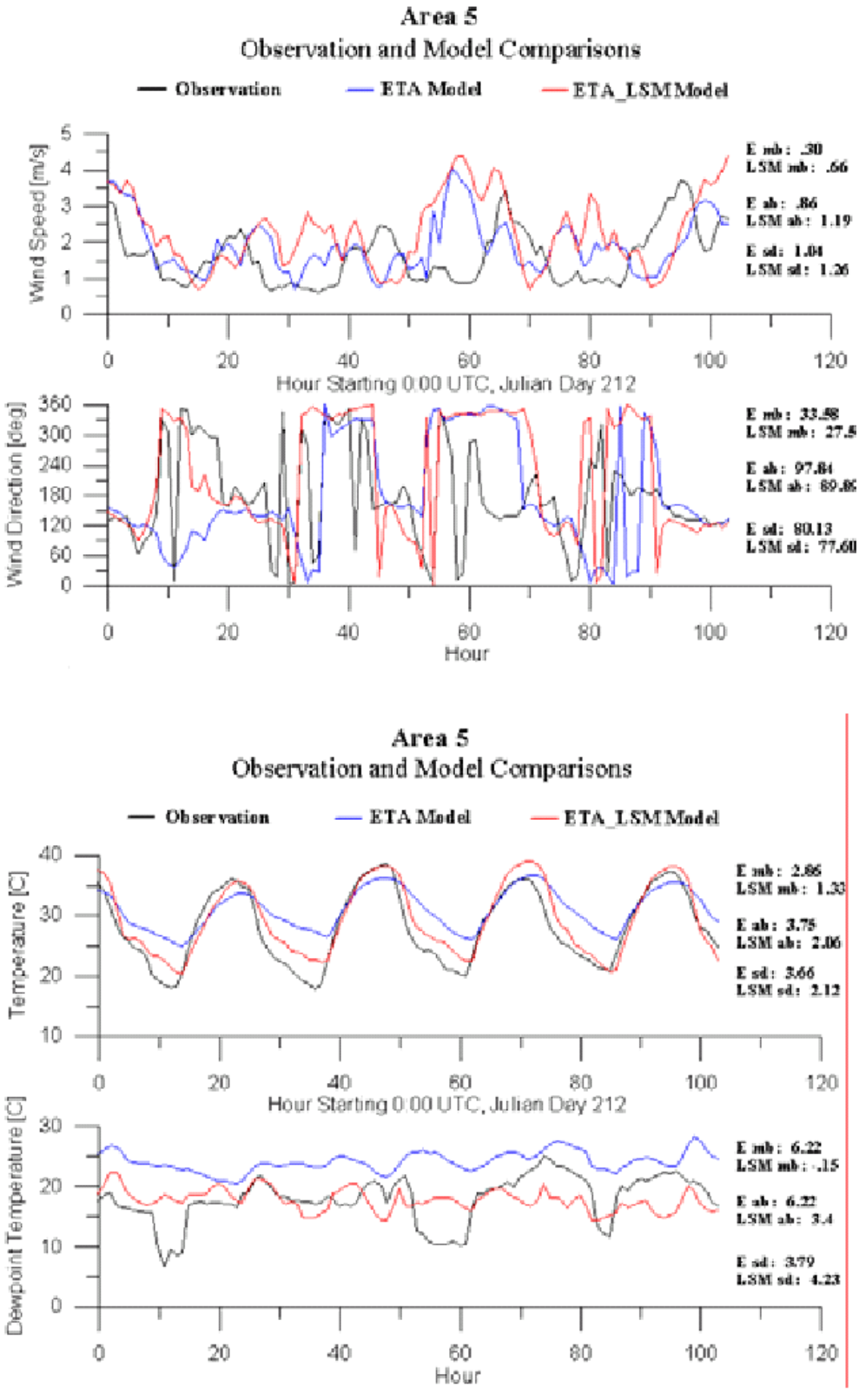

Figure 4-13. Time series of the Area 5 (the northern San Joaquin Valley) average surface meteorology that are arranged from the top panel down: 10-m wind speed (ms-1); 10-m wind direction; 2-m temperature (°C); and 2 m dewpoint temperature (°C). Black line is the observed average, red line is the Run1 average and the blue line is the Run 3 average.

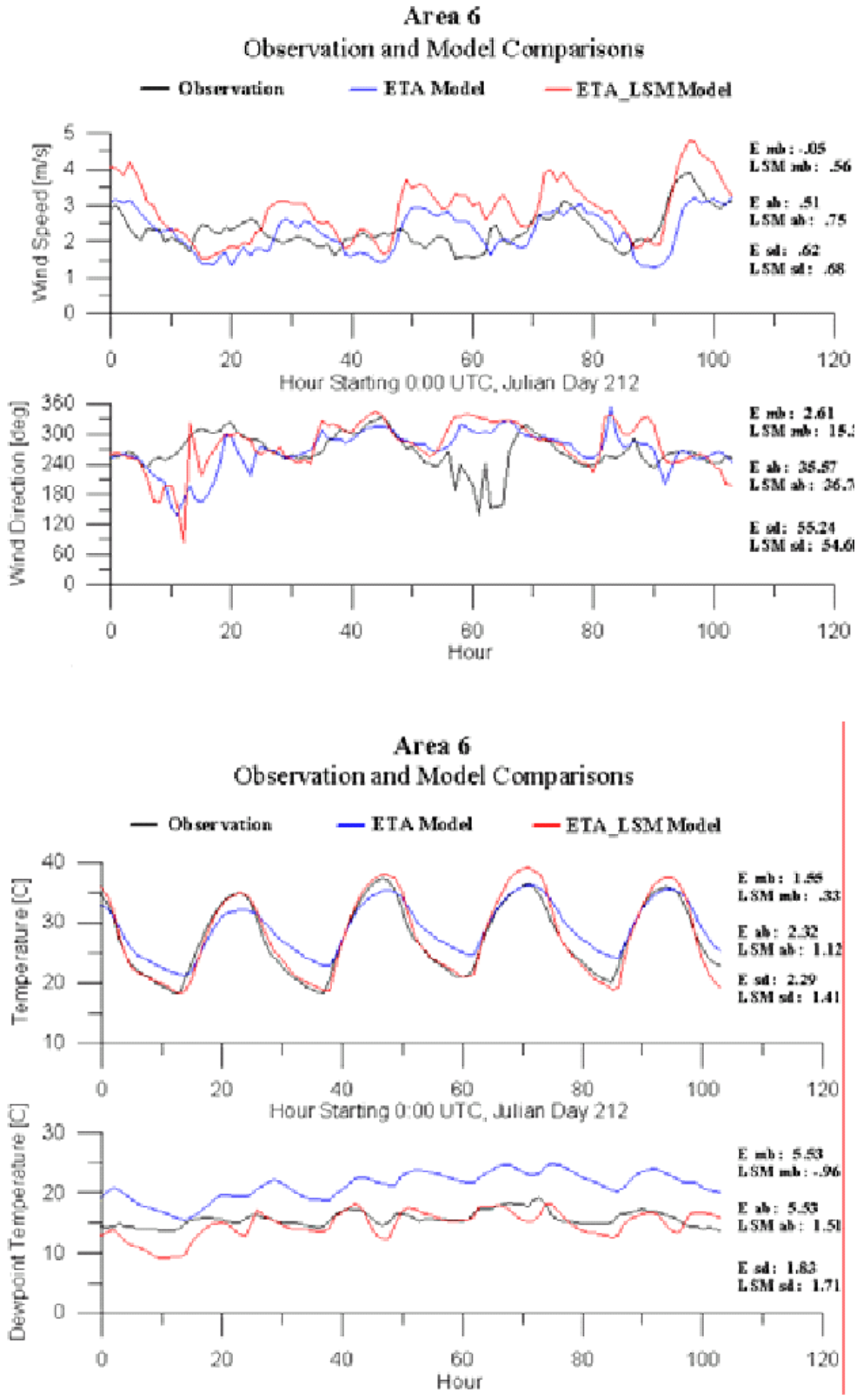

Figure 4-14. Time series of the Area 6 (the central San Joaquin Valley) average surface meteorology that are arranged from the top panel down: 10-m wind speed (ms-1); 10-m wind direction; 2-m temperature (°C); and 2 m dewpoint temperature (°C). Black line is the observed average, red line is the Run1 average and the blue line is the Run 3 average.

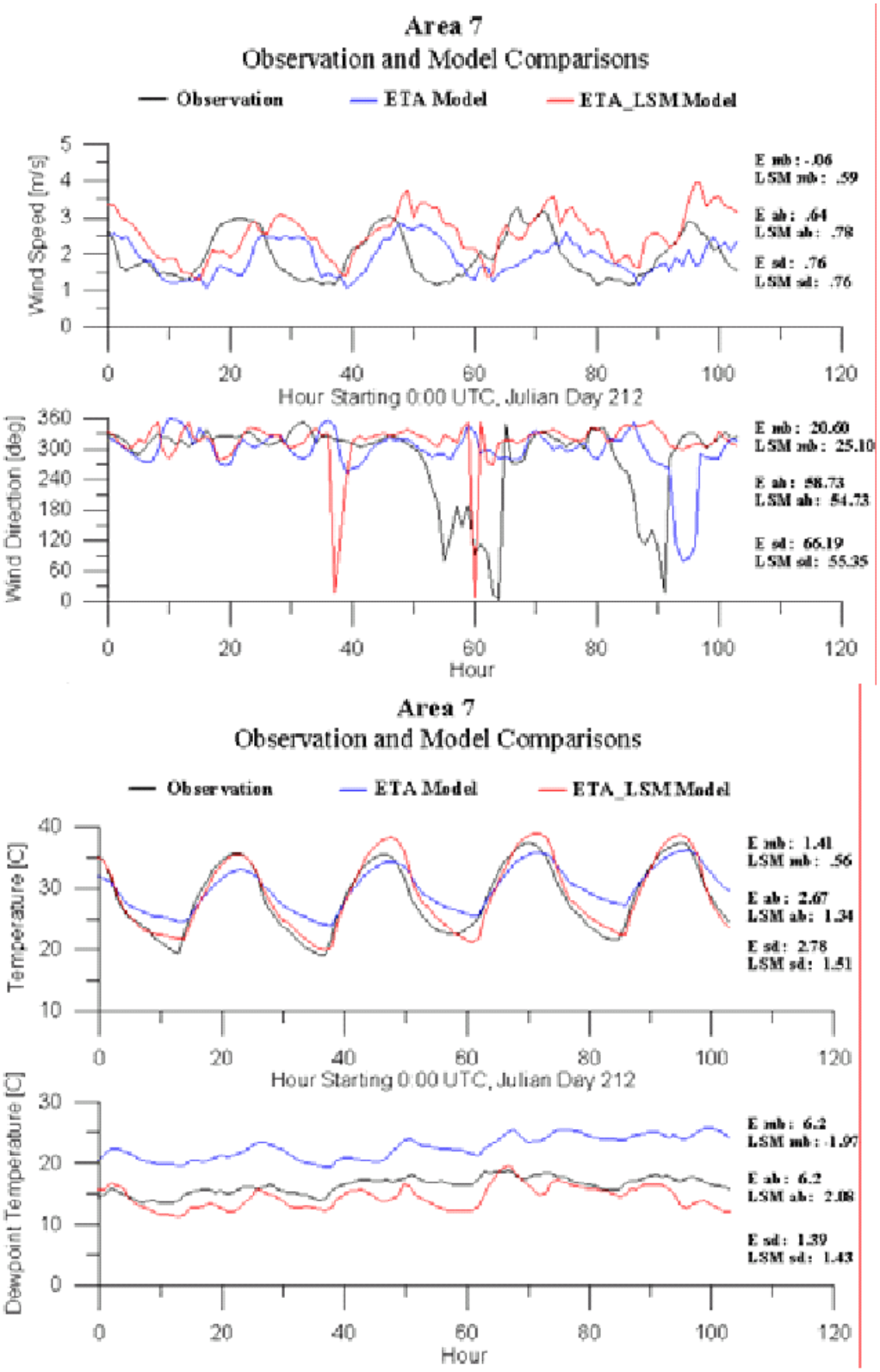

Figure 4-15. Time series of the Area 7 (the southern San Joaquin Valley) average surface meteorology that are arranged from the top panel down: 10-m wind speed (ms-1); 10-m wind direction; 2-m temperature (°C); and 2 m dewpoint temperature (°C). Black line is the observed average, red line is the Run1 average and the blue line is the Run 3 average.

Finally, in Figure 4-16 we show the observed and simulated boundary layer depths, averaged over the central portion of the Central Valley, including Sacramento. Both Run 1 and Run 2 agree quite well with the observed ABL depths, when averaged over the entire IOP. On 31 July (JD213), the second full day shown in the figure, both model simulations also agree very well with the observations. In most other regions of the analysis domain good agreement was found between the observations and model. An exception was for profiler sites immediately inland of the San Francisco Bay Area (Livermore and San Martin sites) where the model frequently produces boundary layer depths that are too low.

Quantitative MM5 Performance Evaluation

ENVIRON carried out a quantitative/statistical performance evaluation of the three MM5 simulations described above. The METSTAT software was utilized to develop daily statistical performance measures for winds, temperature, and humidity. ENVIRON's filtered CCOS meteorological dataset was used to develop the statistics, as described earlier in this section (NWS and AIRS sites only, 10-m winds and 2-m temperature/humidity). These statistics were compared against meteorological performance "benchmarks" as also described earlier in this section. Four areas were analyzed: the SFBA, Sacramento, the Central San Joaquin Valley (including Merced to Visalia, see Figure 4-4), and the southern San Joaquin Valley.

To provide a simpler means of displaying performance against the benchmarks for each parameter and for each day, we employed a particular type of plotting approach (referred to as "soccer goal" plots) that displays the statistical performance of a particular meteorological parameter as a point in a two-dimensional space (e.g., absolute error vs. bias). Furthermore, the "goal" aspect of the plots is denoted by a rectangular region in each error space that denotes performance within the benchmarks; we aim to achieve performance in which the bias/error points fall within the benchmark space.

As discussed above, MM5 performance for winds in the SFBA was quite good for all three runs. Figure 4-17a shows the "soccer goal" plots for this area. While the RMSE for wind speed is within the benchmarks, the wind direction error is slightly larger than we wish to see (30-60 degrees). The relatively high directional error is most likely due to the more complex terrain in this application than seen in many past modeling studies from which the benchmarks were developed. The best performing simulation for winds was Run 2 (Eta PBL, NOAH LSM, FDDA), likely due to nudging to local wind observations. Both Run 1 and Run 3 were similar in terms of wind performance. Figures 4-17b and c show performance for SFBA temperature and humidity, respectively. In this case, Run 3 out performs the other two runs for temperature with acceptable bias but slightly high gross error. Run 2 is the worst temperature performer with large positive bias and error. Humidity performance was rather good for all runs, but again Run 3 tended to perform best.

In Sacramento, all MM5 simulations result in similar wind performance (Figures 4-18a); Run 2 shows the most consistent and best wind performance on a day-to-day basis. Temperature performance is not acceptable for any of the runs, but again Run 2 with FDDA indicates the least amount of under prediction bias (Figure 4-18b). In terms of humidity, the NOAH LSM runs (Runs 1 and 2) are clearly the best performers, with the 5-layer model showing very unacceptable levels of over prediction bias (Figure 4-18c).

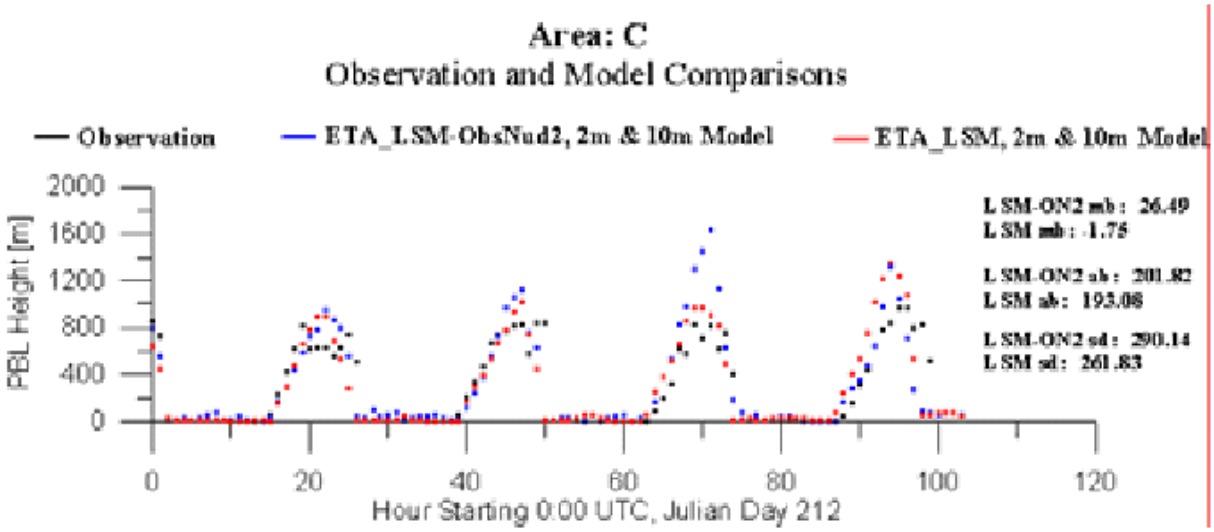

Figure 4-16. The observed and simulated boundary layer depths from Run1 and Run2, averaged over the central portion of the Central Valley.

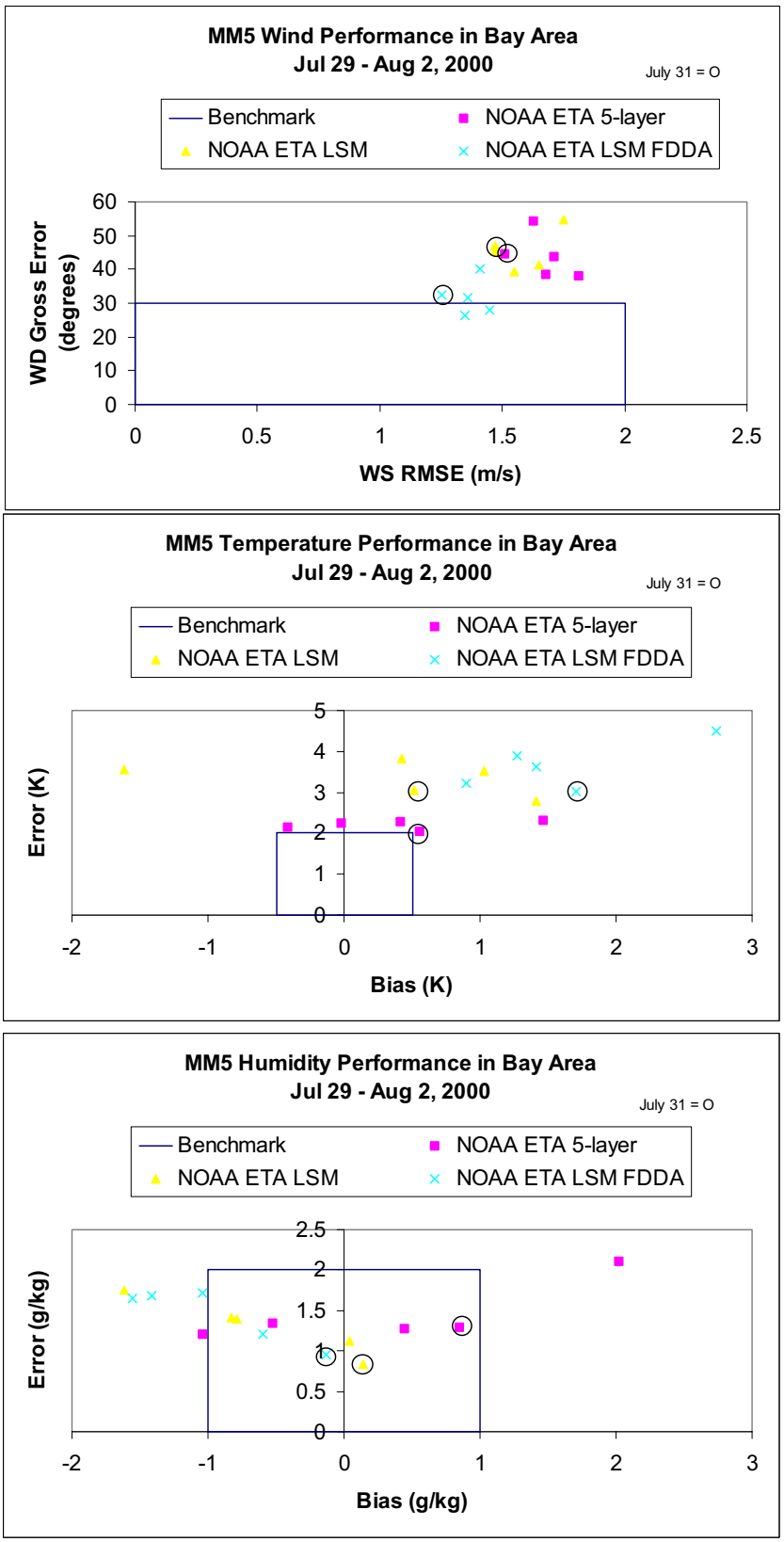

Figure 4-17. MM5 performance for (a) winds, (b) temperature, and (c) humidity in the SFBA analysis region, for Run 1 (yellow triangles), Run 2 (blue stars), and Run 3 (red squares).

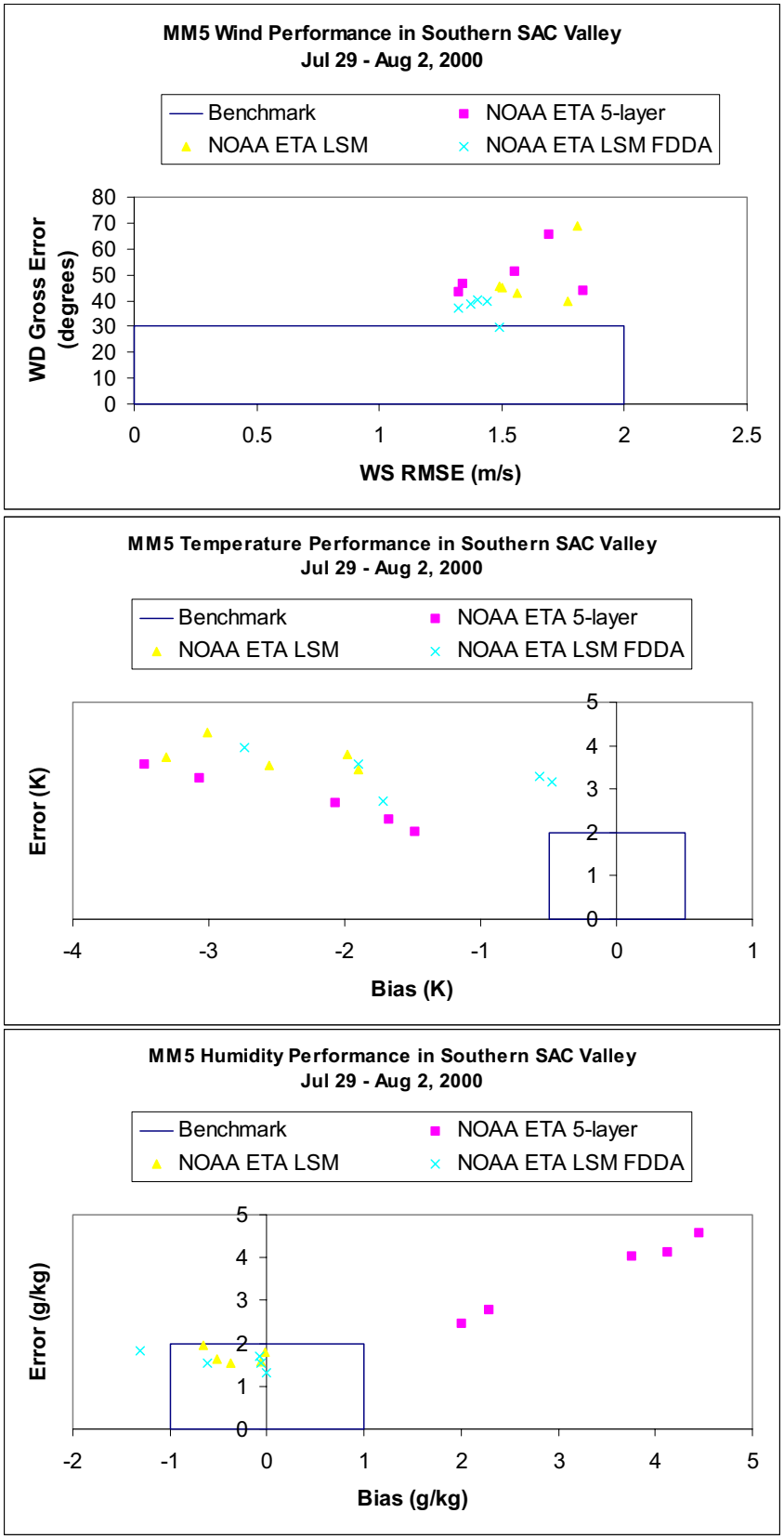

Figure 4-18. MM5 performance for (a) winds, (b) temperature, and (c) humidity in the Sacramento analysis region, for Run 1 (yellow triangles), Run 2 (blue stars), and Run 3 (red squares).

In the central and southern SJV, results are nearly identical to Sacramento for all three meteorological parameters (Figures 4-19a-c and 4-20a-c). The only exception is that humidity performance in the central SJV is unacceptable for all three runs, with Run 3 (5-layer soil model) showing over predictions and Runs 1 and 2 (NOAH LSM) showing under predictions.

Summary from CCOS 2000 MM5 Applications

A case study was carried out in which the output from various MM5 simulations was compared with the wind profiler/RASS and surface observations of wind, temperature, and humidity. The meteorological model was run on a 36-12-4 km one-way nested model domain of 50 vertical levels, with the 4 km domain encompassing the CCOS 2000 field study area. Among various MM5 simulations with different combinations of surface and boundary layer parameterizations, we found that overall the most accurate simulation was produced when using the Eta planetary boundary layer, the NOAH land surface model (LSM), and FDDA.

The direct meteorological comparison between the model simulation and the observations from the CCOS 2000 field experiment indicates that the errors in the simulated low-level winds and surface temperature varied from one area to another, although the model simulated large-scale pattern was in fairly good agreement with the analysis. In terms of time series, the simulated low-level winds were generally in better agreement with the observations in SFBA than in the central valley areas. The opposite was generally true for temperature, where the time traces followed observations better in the central valley areas. However, according to daily-average bias and error statistics, performance was superior in the SFBA for all three meteorological parameters – consistent performance issues were noted for winds, temperature, and humidity throughout the central valley. The use of the NOAH LSM led to more accurate simulations of surface temperature and moisture in the central valley areas. FDDA of the observed winds significantly improved the simulated wind field, and reduced the cold bias in the simulated temperature field. Overall, Run 2 (with NOAH LSM and FDDA) was the best performer for all parameters and in all areas. Good agreement was found between the area average observed and simulated ABL heights except for the area immediately inland such as the San Francisco Bay Area.

MM5 Simulations of the July 1999 Period

MM5 meteorological modeling of the July 9-12, 1999 ozone episode was conducted by the CARB and the BAAQMD. The CARB's modeling was based on their "typical" model configuration that they have employed for several past modeling exercises throughout California. All CARB and BAAQMD simulations were developed on the same CCOS modeling grid horizontally, however for this episode, less vertical resolution was employed (~30 layers for the July 1999 episode vs. ~50 for the CCOS July/August 2000 episode).

The CARB's model configuration utilized the MRF planetary boundary layer scheme in combination with the 5-layer soil model and FDDA observational nudging towards the NWS/CIMIS/RAWS/AIRS meteorological database that CARB compiled in early 2003. Note that the CARB utilized this dataset in the MM5 FDDA scheme before the BAAQMD screened and improved the raw data as described in Section 2. Therefore, this simulation does include a number of questionable observations and mis-located site coordinates.

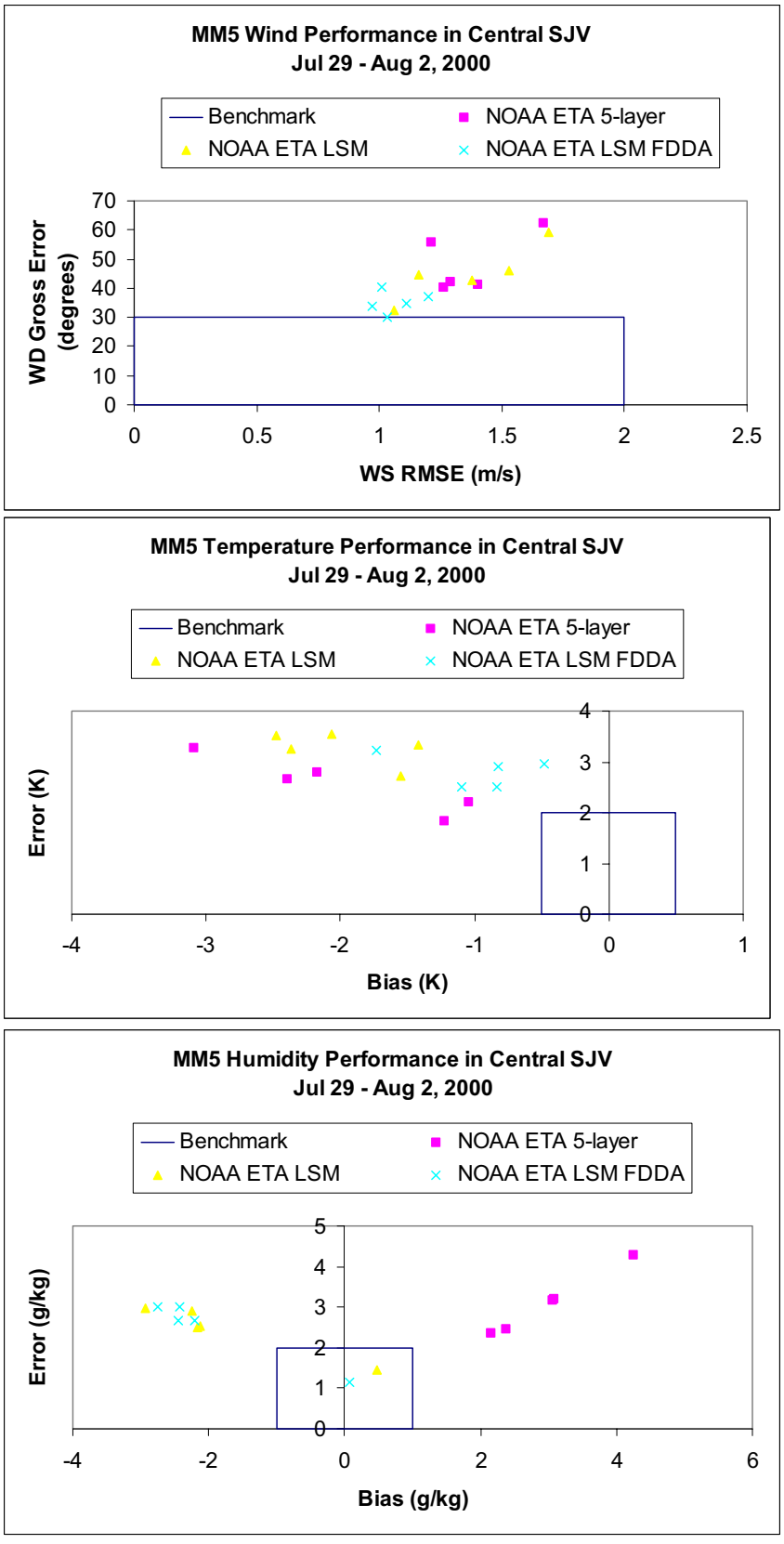

Figure 4-19. MM5 performance for (a) winds, (b) temperature, and (c) humidity in the central SJV analysis region, for Run 1 (yellow triangles), Run 2 (blue stars), and Run 3 (red squares).

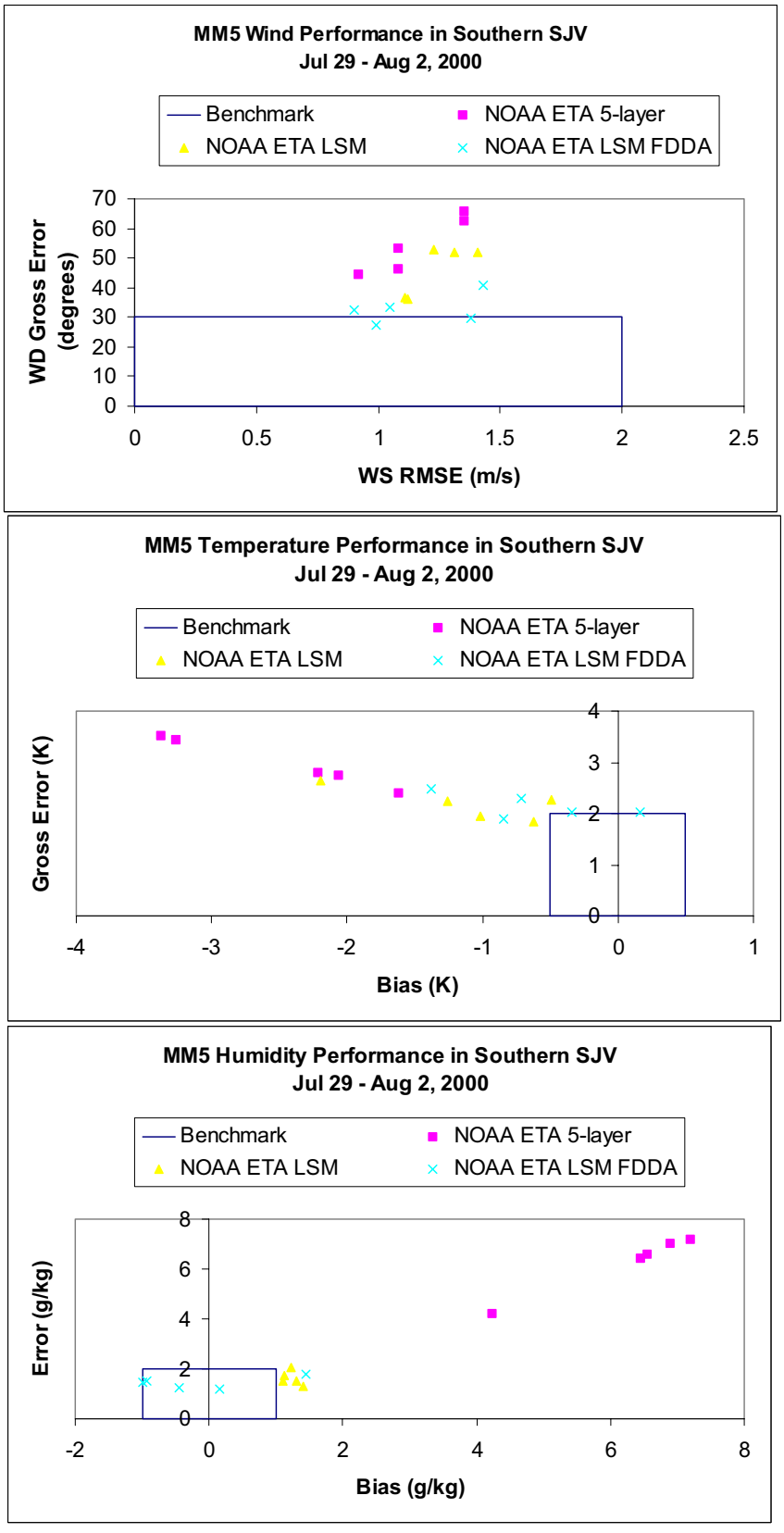

Figure 4-20. MM5 performance for (a) winds, (b) temperature, and (c) humidity in the southern SJV analysis region, for Run 1 (yellow triangles), Run 2 (blue stars), and Run 3 (red squares).

The BAAQMD undertook two initial sensitivity runs with MM5 using the CARB configuration. First, the model was run with no FDDA whatsoever to provide a gauge for assessing the impact of observational FDDA in the CARB simulation. Second, the BAAQMD performed the same observation-nudging simulation as the CARB, but provided the model with their screened/ improved meteorological dataset. Third, grid/analysis nudging FDDA was employed (replacing the observational FDDA approach), in which MM5 was supplied 4-km analysis fields from the NCEP/NCAR's routine Eta Data Assimilation System (EDAS) products. Analysis nudging provides three-dimensional data assimilation over the entire modeling grid, but BAAQMD elected to nudge only above 700 mb (~3000 m) in order to ensure that the synoptic scale forcings were properly represented. The basis for this approach assumes that properly capturing large-scale weather patterns aloft will lead to appropriate boundary layer and mesoscale circulations in the model, which are so important for resolving chemistry, mixing, and transport in the complex terrain of the CCOS grid.

The MM5 results from all three simulations were processed through the METSTAT program for subsequent quantitative performance evaluation. As in the analyses of the CCOS 2000 MM5 evaluation, the model results were compared to a reduced observational dataset comprising of just NWS and AIRS sites to ensure 10-m winds and 2-m temperatures. Performance statistics and site-averaged time series were calculated for four regions: the SFBA, Sacramento, central SJV, and southern SJV (see Figure 4-4). Since the CARB-compiled meteorological dataset did not include any humidity measures, performance for this parameter was omitted from the analysis.

Figure 4-21 provides site-averaged time series of winds and temperatures for the SFBA region. Wind speeds were generally under predicted over the simulation period, particularly for the key days of interest (July 11 and 12). Little difference is noted among most simulations, except for the analysis FDDA run, which generally performed quite well for wind speed. However, the opposite is true for wind direction, with the analysis FDDA run performing much worse over the key days than the other simulations. Observational nudging appears to help the directional alignment in the SFBA (an expected result) – the under prediction of speed, however, is likely due to nudging toward many sites with probe heights much lower than 10 m, and gauging results against speeds from probes at 10 m. Time series of temperature shows that the model performed well in replicating the diurnal wave in most simulations, except possibly the analysis FDDA run, which shows the strongest deviations from the other runs and overall worst performance.

Soccer goal plots of daily performance for winds and temperature are provided in Figure 4-22. The original CARB run is the best overall performer for winds. The analysis FDDA run shows the most directional error of the four. Temperature performance is consistent among the runs, except again the analysis FDDA run varies widely over the period. None show acceptable performance.

Site-averaged time series for Sacramento (Figure 4-23) show the classic problem with the MM5's MRF scheme; the diurnal phase lag of wind speed. Besides generally under predicting speed, the timing of daily maxima and minima are shifted by 6-8 hours. Most runs lead to consistent results, except for the analysis FDDA run, which leads to an over prediction in wind speeds (note the phase shift is not affected). Significant differences among the runs are seen in the wind direction performance. None of the runs seem to adequately capture the mean directional trend, possibly because the observations are light and variable and all meteorological models have difficultly replicating conditions under weakly forced patterns. For temperature, all

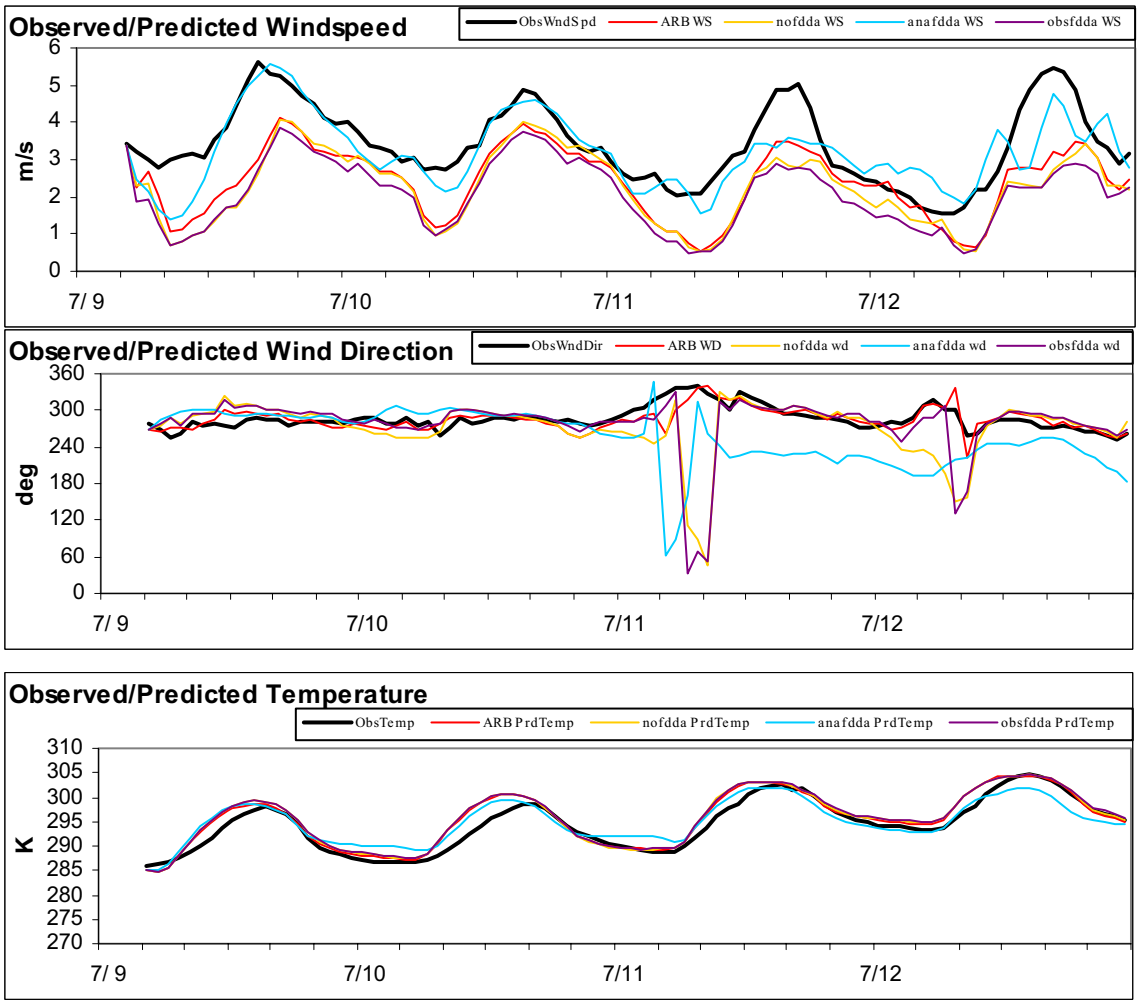

Figure 4-21. Site-averaged time series of wind speed, direction, and temperature for the SFBA over the July 9-12, 1999 modeling period. Observations are shown in bold black, and various MM5 simulations are shown as thinner colored traces.

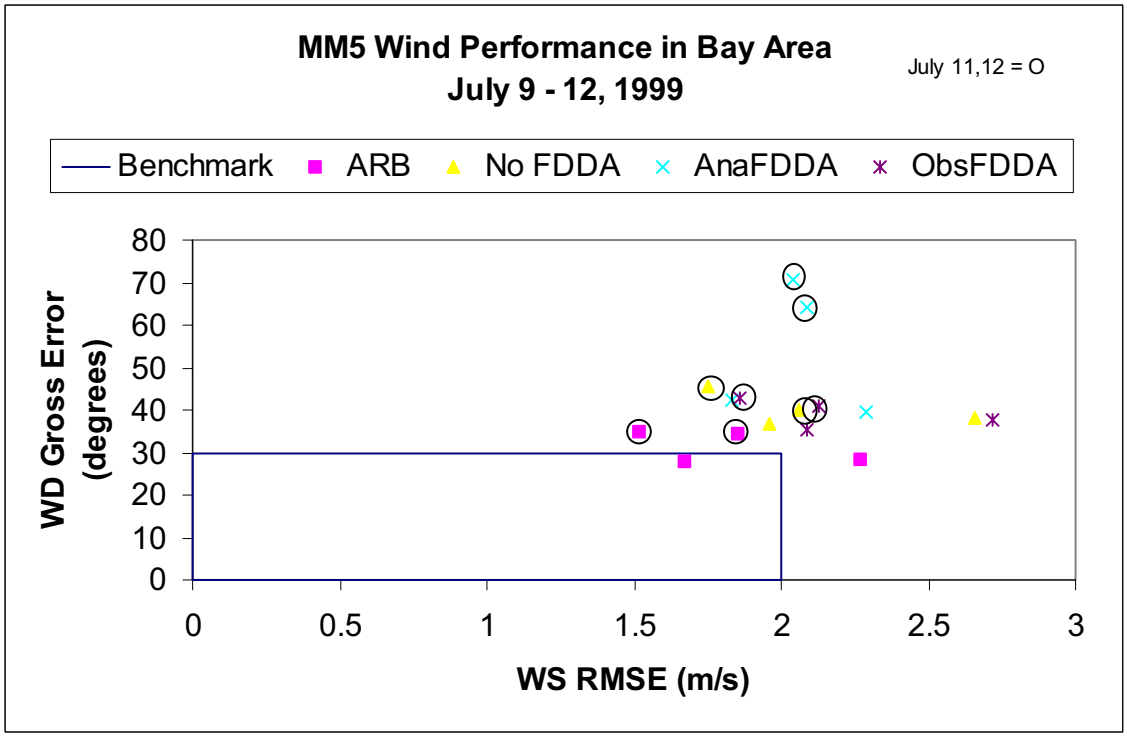

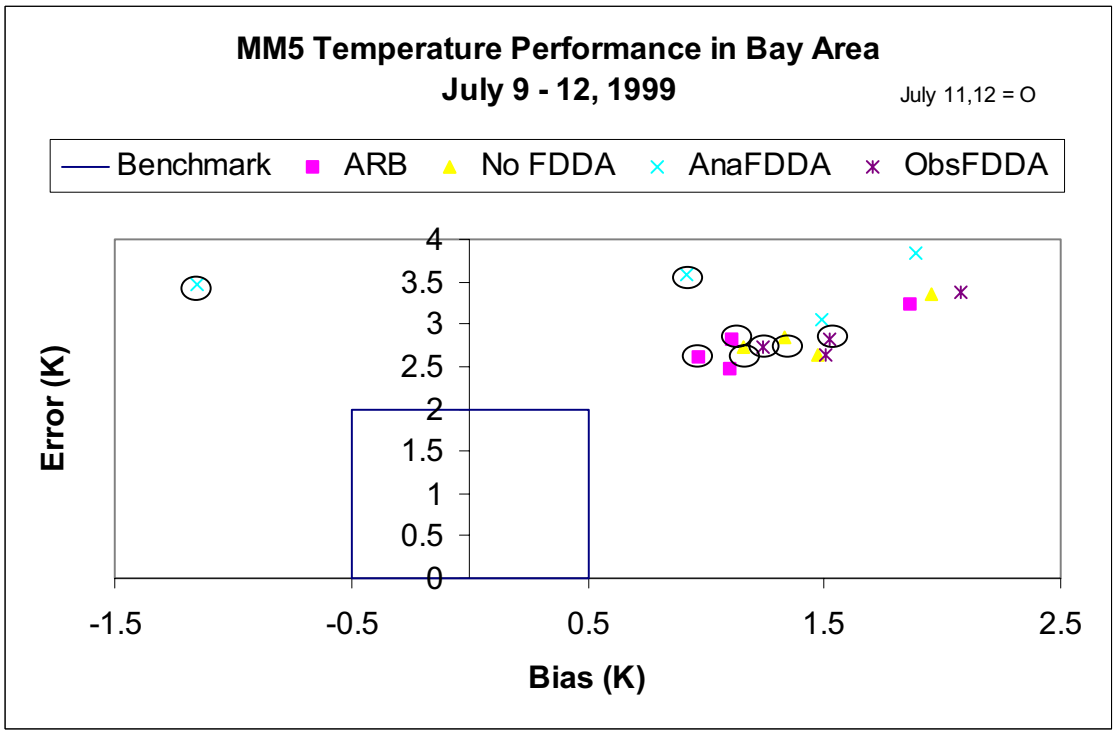

Figure 4-22. MM5 performance for (a) winds and (b) temperature in the SFBA analysis region. Circled points indicate performance specifically on July 11 and 12.

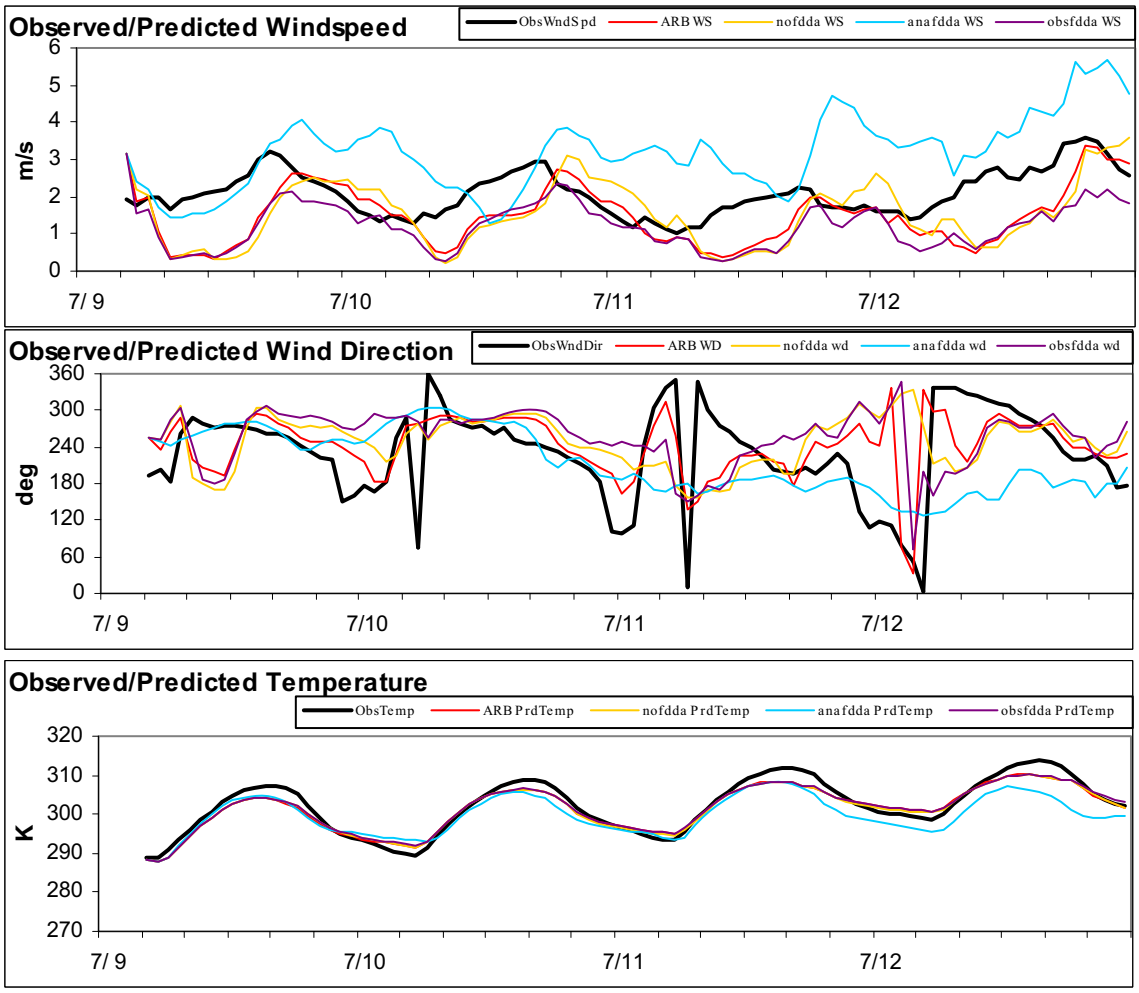

Figure 4-23. Site-averaged time series of wind speed, direction, and temperature for the Sacramento area over the July 9-12, 1999 modeling period. Observations are shown in bold black, and various MM5 simulations are shown as thinner colored traces.

simulations under predicted the peak temperatures every afternoon, but perform acceptably at other times.

Daily performance for winds (Figure 4-24) again indicate that the original CARB simulation is best overall, although none are acceptable relative to the benchmarks. The analysis FDDA run is particularly poor. The same is true for temperature, and the under prediction bias is clearly obvious.

Performance for the central and southern SJV (Figures 4-25 through 4-28) show all of the same characteristics as Sacramento, including: (1) the wind speed phase lag and over predictions for the analysis FDDA run; (2) wide variation in wind direction among the runs on July 11 and 12, with none replicating the mean observations particularly well; (3) under predicted daytime temperatures in all runs, with particularly bad performance in the southern SJV; (4) the best daily statistical wind performance for the original CARB run and the worst for the BAAQMD analysis FDDA run; and (5) dramatic and unacceptable daily under prediction performance for temperature in all runs.

The BAAQMD noted that use of the Eta PBL scheme in the CCOS 2000 simulations did not lead to the wind speed phase lag problems evident in the MRF results described above. Furthermore, it was noted that the MRF generates overly deep boundary layer depths, which were not the case using the Eta PBL. Finally, it was realized that the poor temperature performance in the central valley could be improved with the use of a land surface model (LSM), as evidenced from previous BAAQMD simulations for July/August 2000. The BAAQMD carried out two additional MM5 runs in which they replaced the MRF with the Eta PBL scheme, and replaced the 5-layer soil model with the NOAH LSM. Both runs were otherwise configured similarly to the BAAQMD's non-FDDA run presented above. Results were only available from the Eta case in time for this report.

Figure 4-29 shows the region-average wind speed and temperature time series for the central SJV (one of the areas indicating a strong phase lag) for the Eta PBL case. A strong improvement in the wind speed performance is clearly evident relative to the original non-FDDA case. However, wind direction and temperature are not significantly impacted; usually these are more responsive to observational FDDA and the use of an LSM, respectively. Soccer-goal plots comparing these two cases (Figure 4-30) show a remarkable improvement in daily wind speed error, but no improvement in direction and an actually worsening of daily temperature performance.

Summary from July 1999 MM5 Applications

The CARB and BAAQMD conducted MM5 modeling of the July 9-12, 1999 period using a consistent model configuration based on applications conducted by the CARB in the past. This included the use of the MRF PBL scheme, the 5-layer soil model, and various incarnations of FDDA. Horizontally, MM5 was applied on the CCOS modeling domain, but only ~30 vertical layers were specified in the July 1999 simulations. The CARB simulation included observational FDDA to the original unscreened meteorological dataset that they compiled in early 2003. The BAAQMD applications tested the model with no FDDA whatsoever, analysis nudging toward EDAS, observational nudging toward the screened/improved observation dataset, and runs testing the impacts from using the Eta PBL scheme and the NOAH LSM.

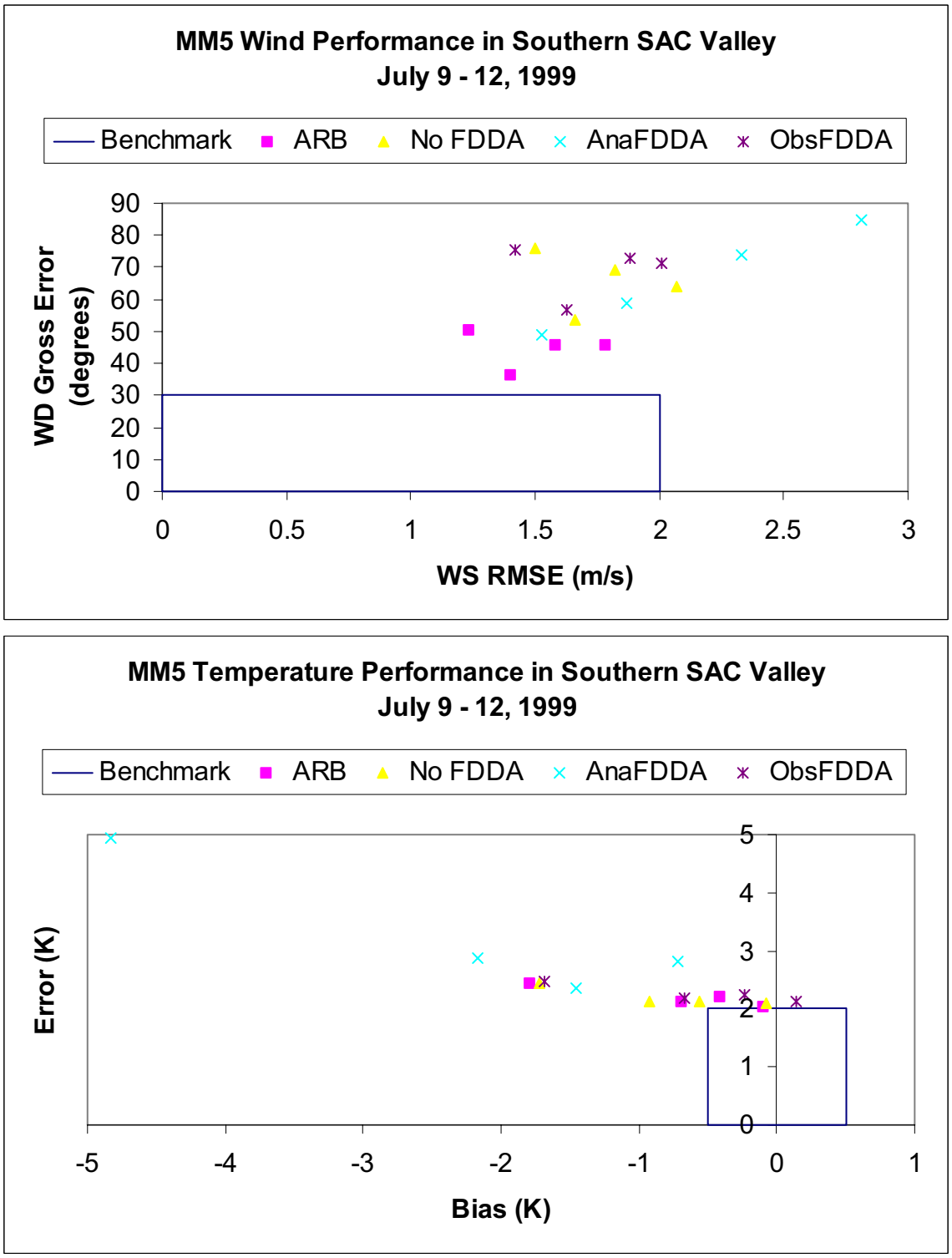

Figure 4-24. MM5 performance for (a) winds and (b) temperature in the Sacramento analysis region.

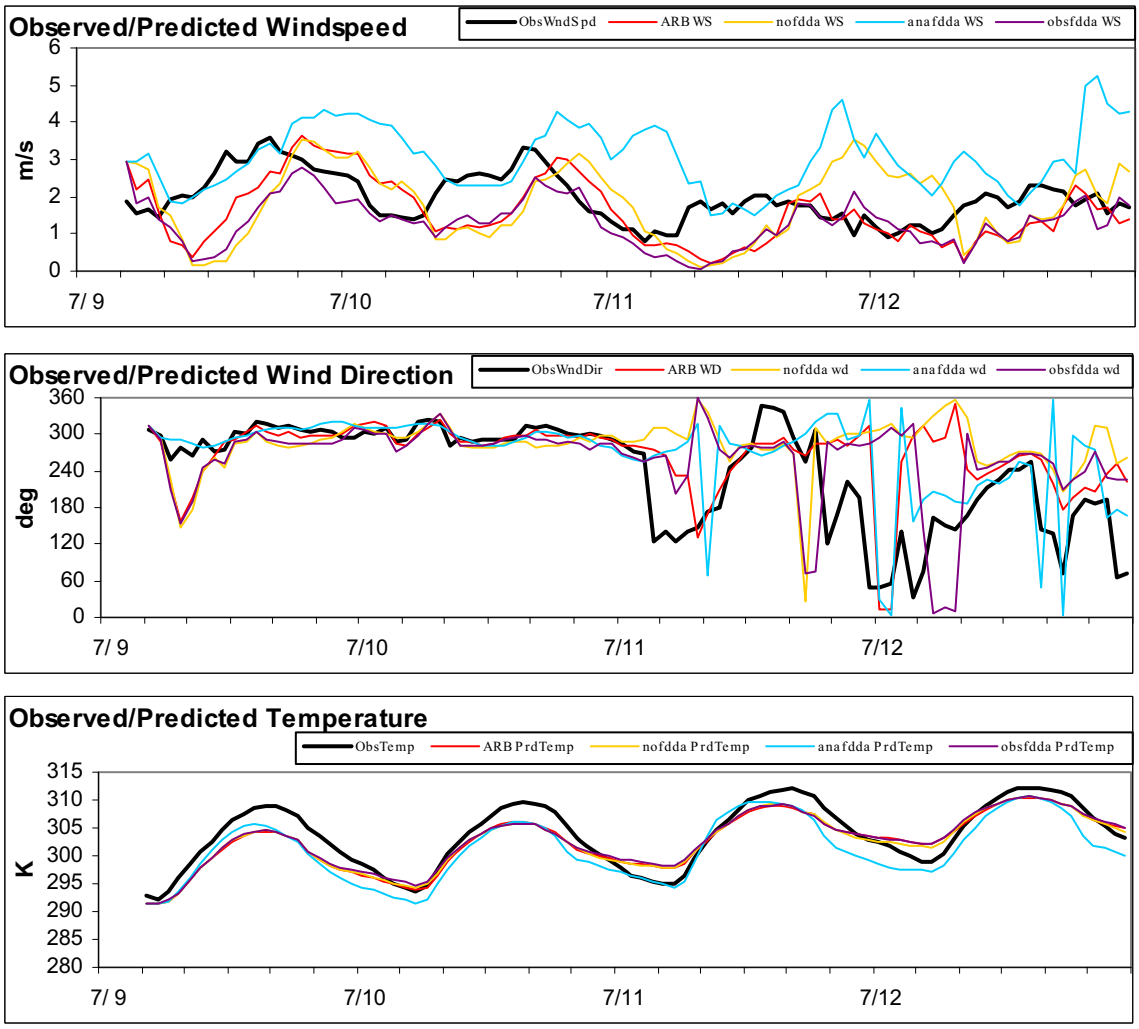

Figure 4-25. Site-averaged time series of wind speed, direction, and temperature for the central SJV area over the July 9-12, 1999 modeling period. Observations are shown in bold black, and various MM5 simulations are shown as thinner colored traces.

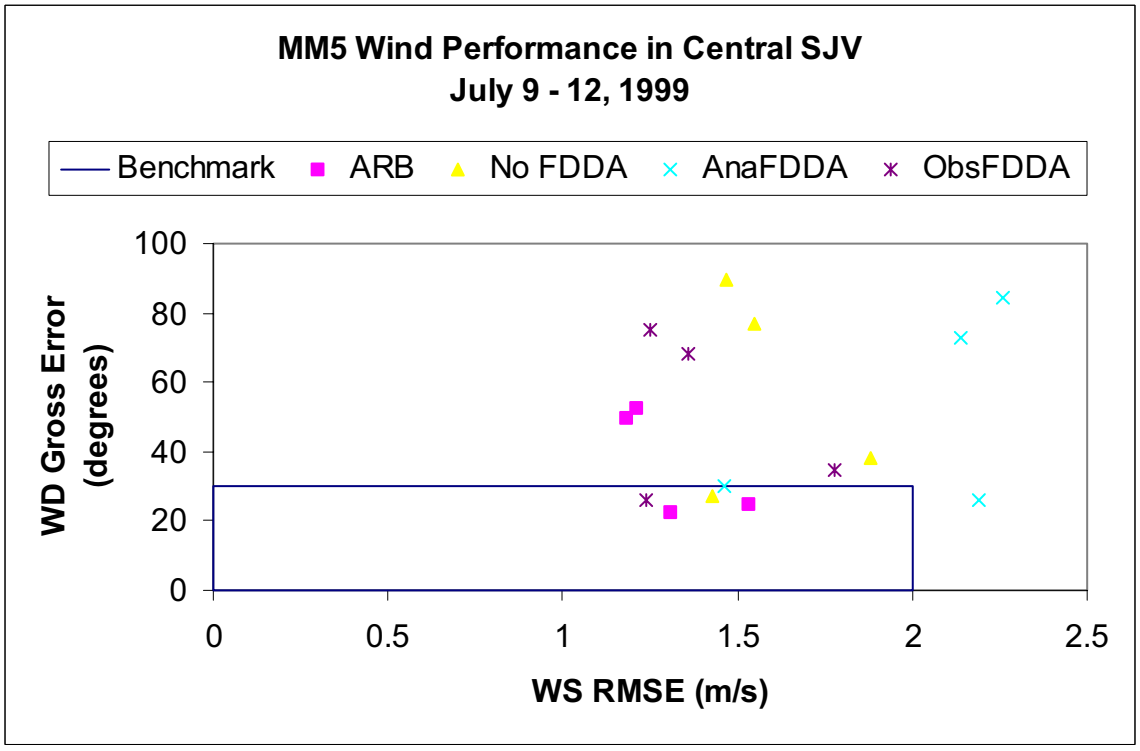

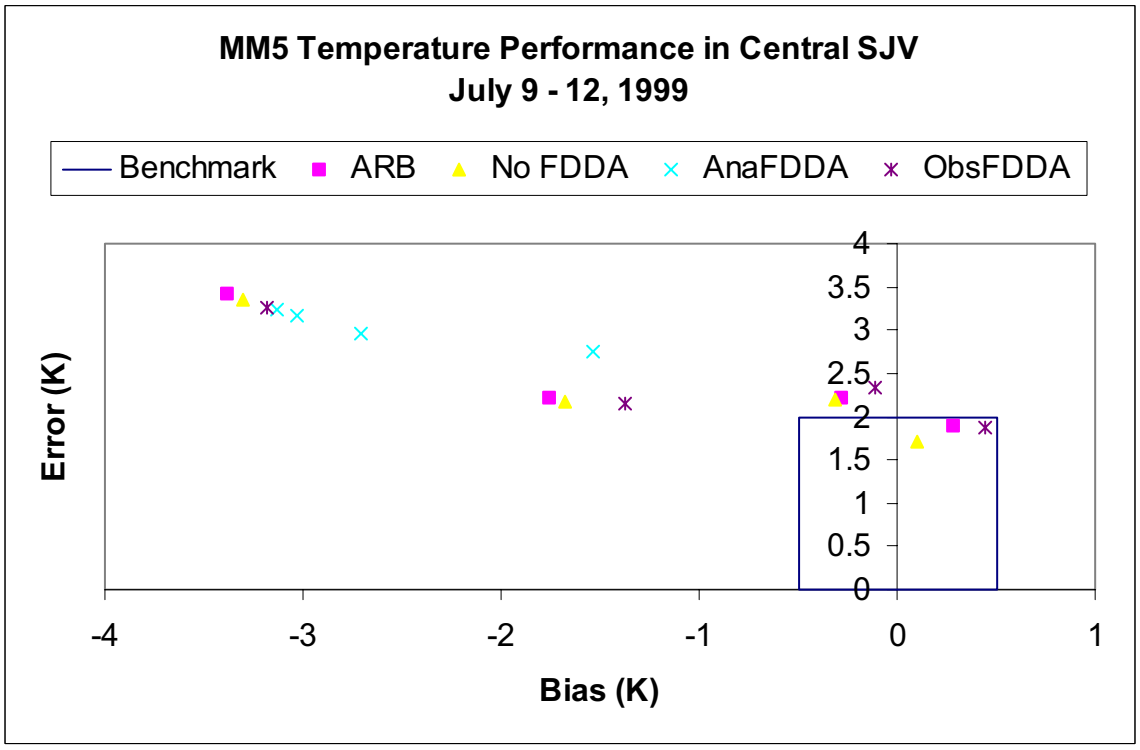

Figure 4-26. MM5 performance for (a) winds and (b) temperature in the central SJV analysis region.

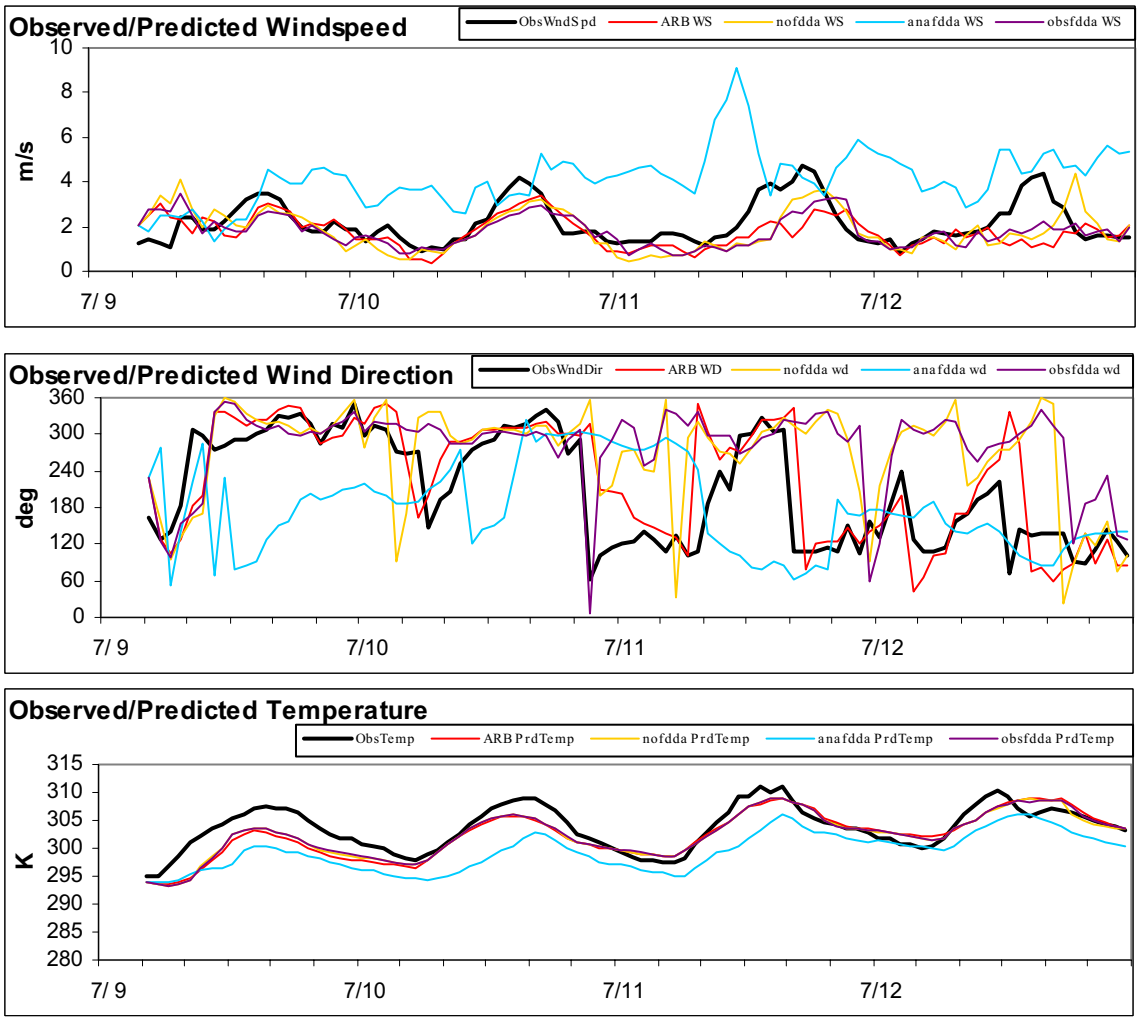

Figure 4-27. Site-averaged time series of wind speed, direction, and temperature for the southern SJV area over the July 9-12, 1999 modeling period. Observations are shown in bold black, and various MM5 simulations are shown as thinner colored traces.

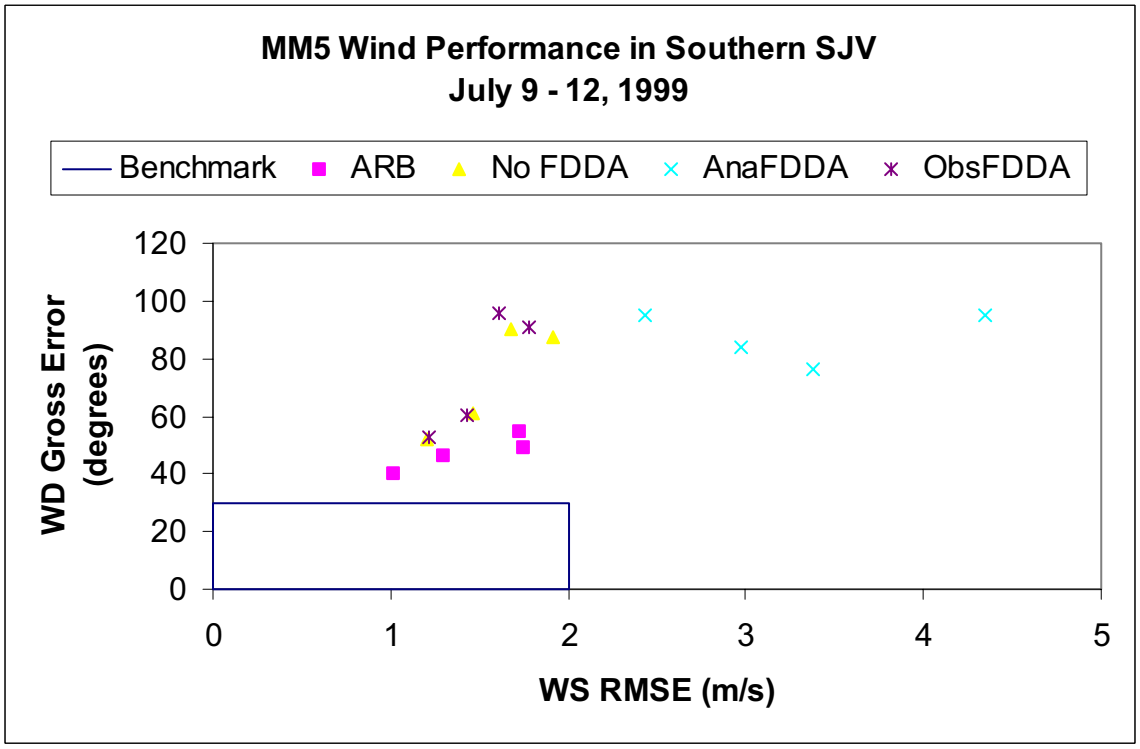

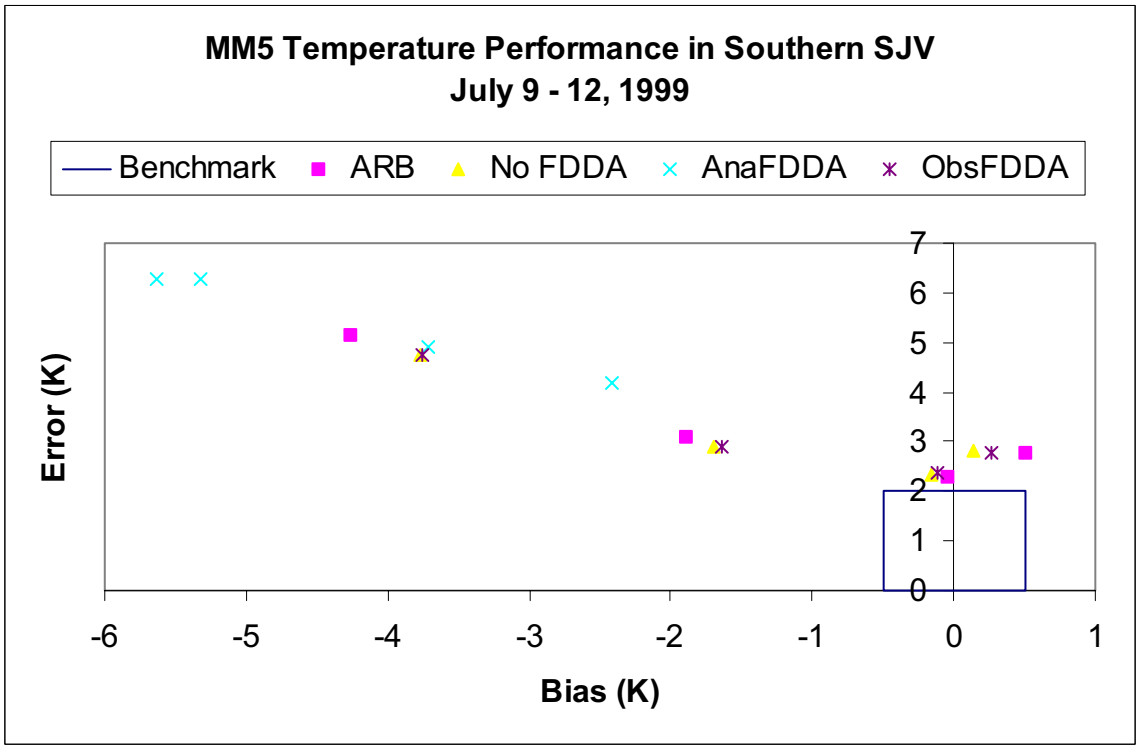

Figure 4-28. MM5 performance for (a) winds and (b) temperature in the southern SJV analysis region.

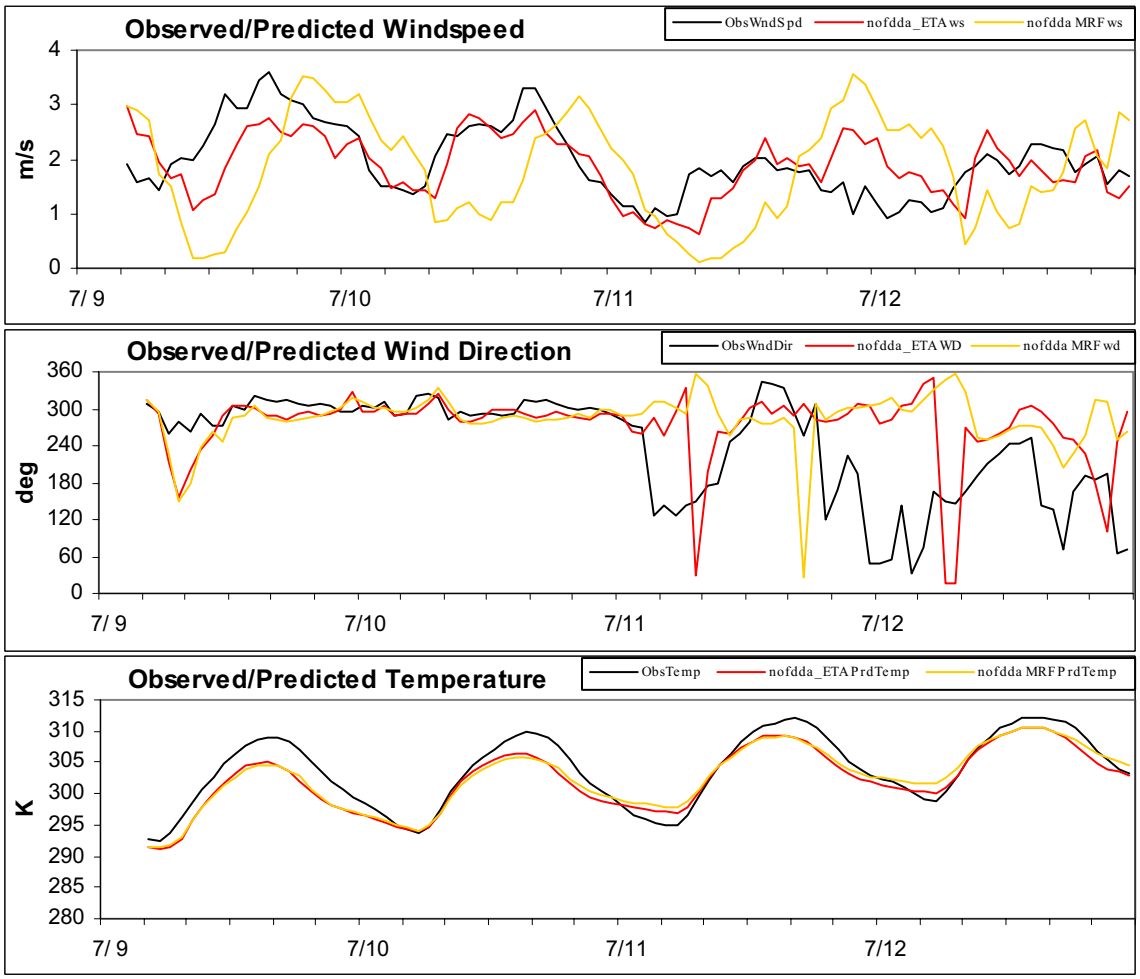

Figure 4-29. Site-averaged time series of wind speed, direction, and temperature for the central SJV area over the July 9-12, 1999 modeling period. Observations are shown in bold black, the MM5 Eta PBL run is shown in red, and the MM5 MRF PBL run is shown in yellow.

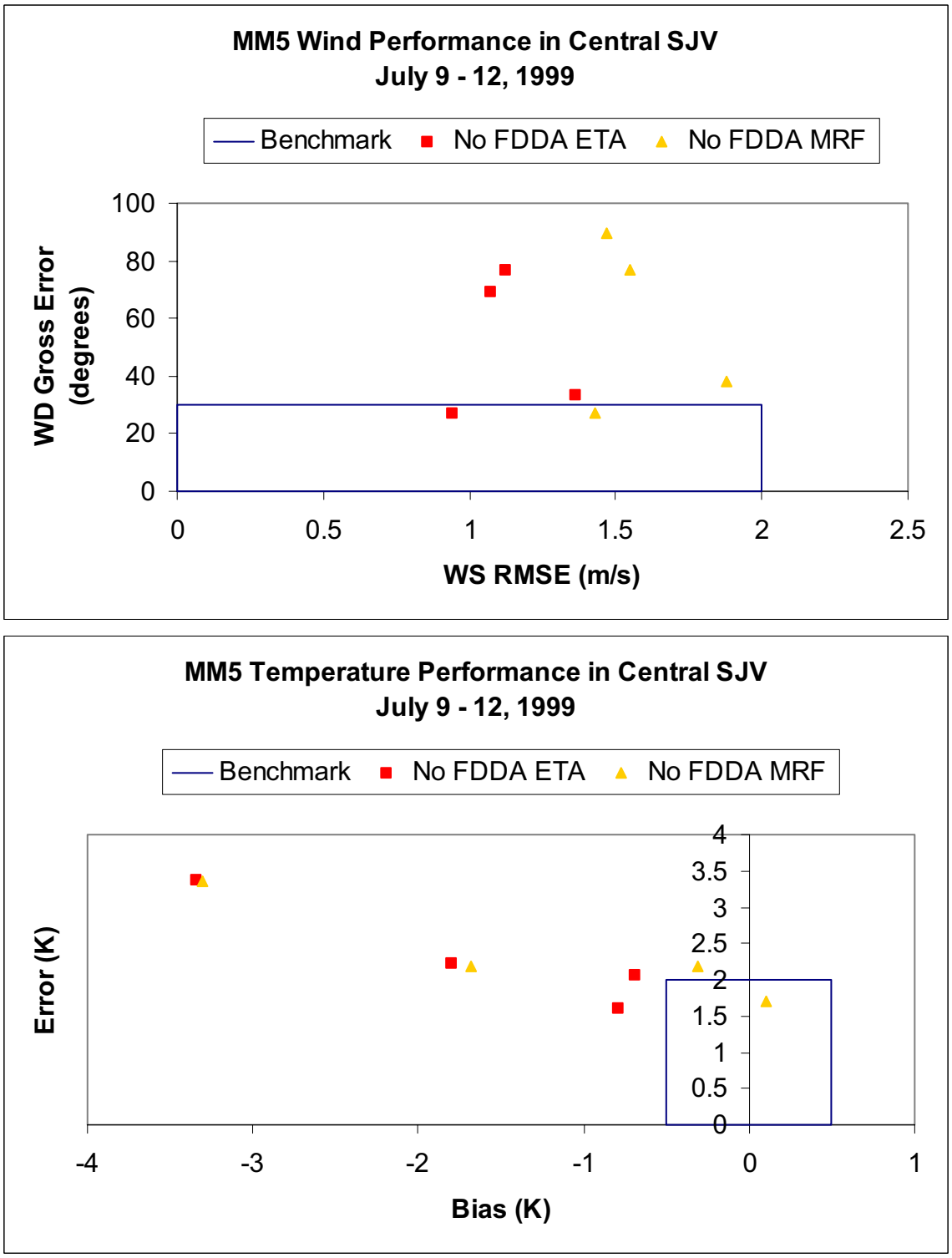

Figure 4-30. MM5 performance for (a) winds and (b) temperature in the central SJV analysis region for the BAAQMD MM5 Eta and MM5 MRF simulations.

Graphical and statistical results show that the original CARB run consistently performed better than any BAAQMD FDDA sensitivity test. Analysis nudging improves wind speed performance in the SFBA, but it is clearly the worst run in all other respects. The MRF "phase-lag" problem was clearly evident for areas in the central valley. Wind direction performance especially was unacceptable on July 11-12 in the central valley. The SFBA was too warm and the central valley (particularly the southern SJV) was too cool in all runs. Humidity was not evaluated due to lack of data, but the cool bias in the central valley was likely associated with a positive moisture bias as seen in the CCOS 2000 modeling results.

BAAQMD tests using the Eta PBL fixed the phase-lag problem associated with the MRF PBL scheme. However, no significant impacts were seen for direction, and a slight degradation of temperature performance was seen in the central valley. Results from tests using the NOAH LSM were not available in time for this report.

The "best" MM5 simulations for this episode are only moderately acceptable relative to performance benchmarks established from a vast array of meteorological modeling conducted across the country. This may be as much related to the complex terrain and high model resolution over such a vast area as to the quality of the data used in the performance evaluation. As will be discussed in Section 7, the best MM5 simulation does not always lead to the best CAMx performance. Remaining issues include:

- Proper temperature performance leads to overly high SFBA winds, and vice-versa;
- There may be a need for more terrain-induced "drag" on the winds, including proper resolution of terrain elevation in the modeling grid, valley channeling, and effects of unresolved terrain features that add to surface roughness;
- The default MM5 surface roughness values as a function of land cover category are now known to be too low; tests in other studies outside of California have shown improved results when higher values for roughness are employed.